

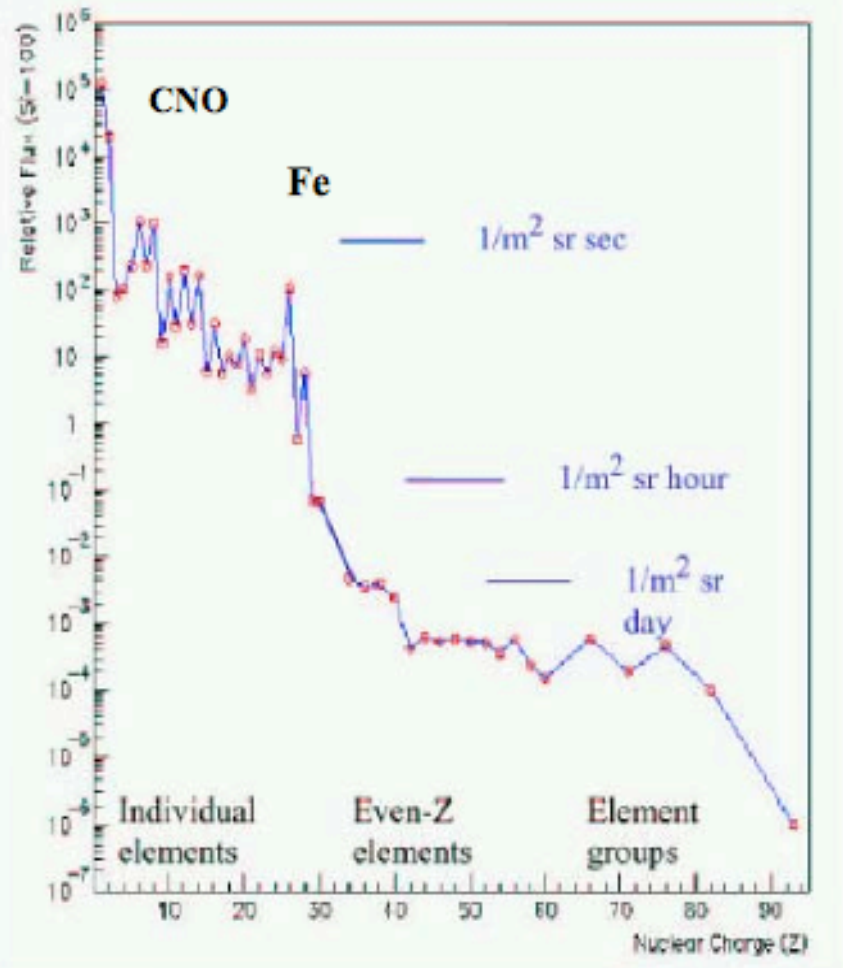
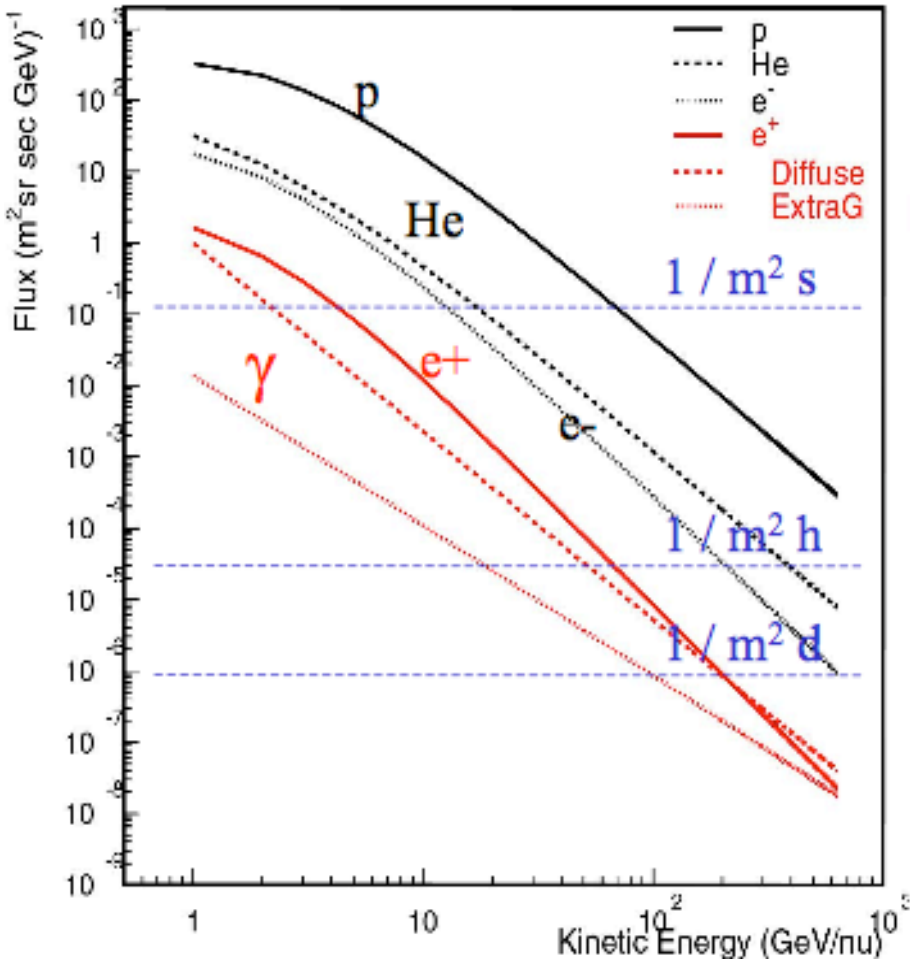
Astrofisica e particelle elementari

aa 2007-08

Lezione 19

Bruno Borgia

RC: particelle e nuclei



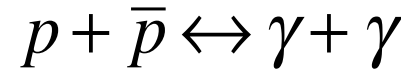
ANTIMATERIA

L'ipotesi del Big Bang è in accordo con

- l'espansione dell'universo
- la nucleosintesi primordiale
- la radiazione cosmica di corpo nero

L'assenza di antimateria non ha un fondamento certo secondo le conoscenze attuali.

Nell'universo primitivo quando $kT > m_{\text{adroni}}$



Barioni, antibarioni e fotoni si trovavano in equilibrio termico.

Con l'espansione e il raffreddamento, i fotoni anche nella coda dello spettro di radiazione di corpo nero non hanno energia per creare coppie di nucleoni-antinucleoni. La densità di p e anti-p è così bassa che non si annichilano più. La temperatura critica è $kT \approx 20 \text{ MeV}$.

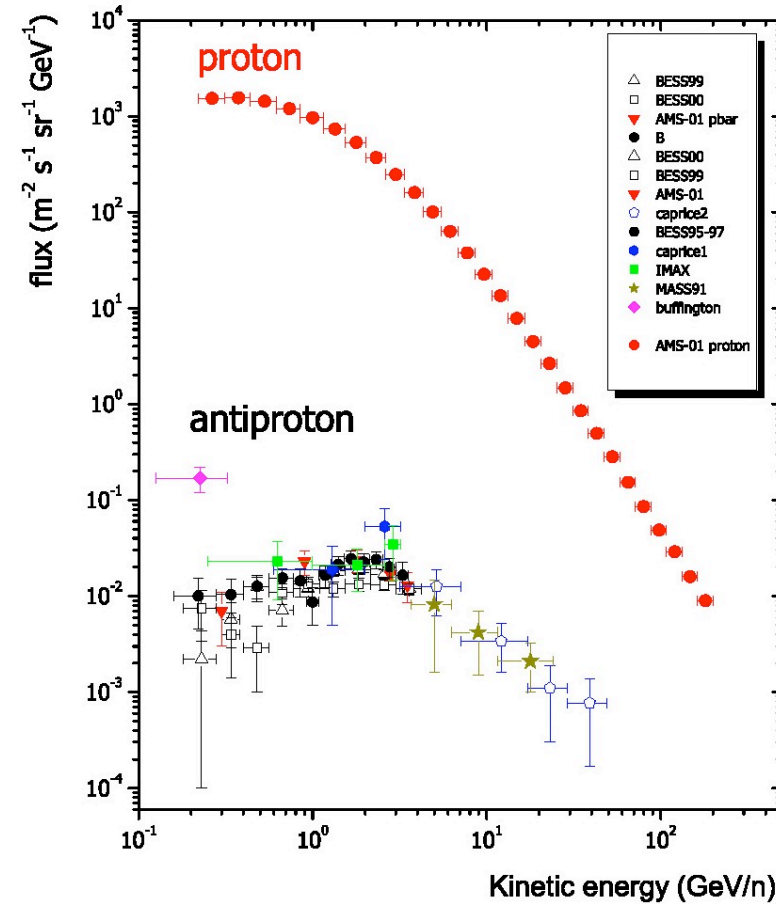
La densità di barioni e antibarioni susseguente, rispetto alla densità di fotoni, si mantiene costante e si calcola

$$\frac{N_B}{N_\gamma} = \frac{N_{\bar{B}}}{N_\gamma} \approx 10^{-18}$$

ANTIMATERIA?

Al contrario i rapporti
sperimentali sono

$$\frac{N_B}{N_\gamma} \approx 10^{-9}; \quad \frac{N_{\bar{B}}}{N_B} < 10^{-4}$$



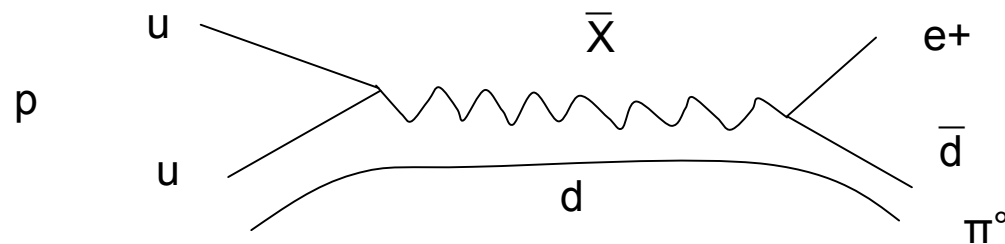
$$\frac{\Phi_{\bar{p}}}{\Phi_p} \sim 10^{-4} - 10^{-5}$$

BARIOGENESI

Le condizioni per ottenere asimmetria materia/antimateria (Sakharov 1967), sono:

- violazione del numero barionico; *limite vita media del $p > 10^{33}$ anni*
- deviazione dall'equilibrio termico nel plasma primordiale; possibile e favorevole se $T \approx m$
- violazione di C e CP; *misurata nel decadimento del K e del B.*

GUT (Grand Unified Theories), ad esempio SUSY, forniscono un meccanismo diretto per la violazione di B tramite lo scambio di un bosone supersimmetrico X:



BARIOGENESI - GUT

- E' permessa la violazione del numero barionico B e del numero leptonico L in modo tale che la carica totale sia conservata, $(B-L) = \text{cost}$
- I bosoni supersimmetrici X e Y presenti alla scala temporale $t = 10^{-40}$ s decadono in due ipotetici canali con barioni B_1 e B_2 .
- Siano x e \bar{x} i rapporti di decadimento di X e \bar{X} in B_1
- Si ha

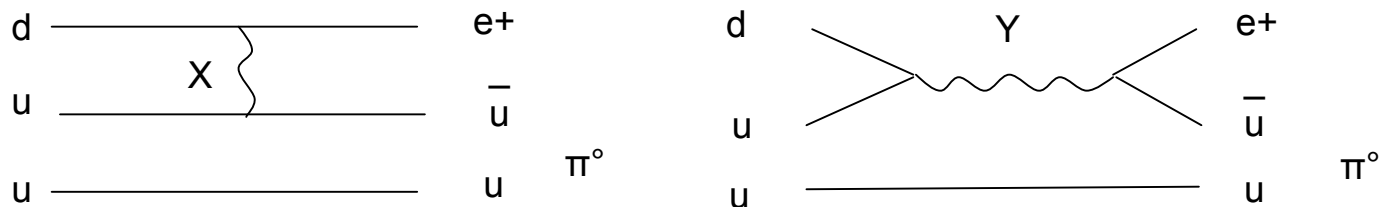
$X \rightarrow xB_1$	$X \rightarrow (1-x)B_2$
$\bar{X} \rightarrow \bar{x}B_1$	$\bar{X} \rightarrow (1-\bar{x})B_2$
- L'asimmetria barionica sar  quindi

$$A = xB_1 - \bar{x}B_1 + (1-x)B_2 - (1-\bar{x})B_2 = (x - \bar{x})(B_1 - B_2)$$

- La violazione di B assicura $B_1 \neq B_2$
- La violazione di CP assicura $\bar{x} \neq x$

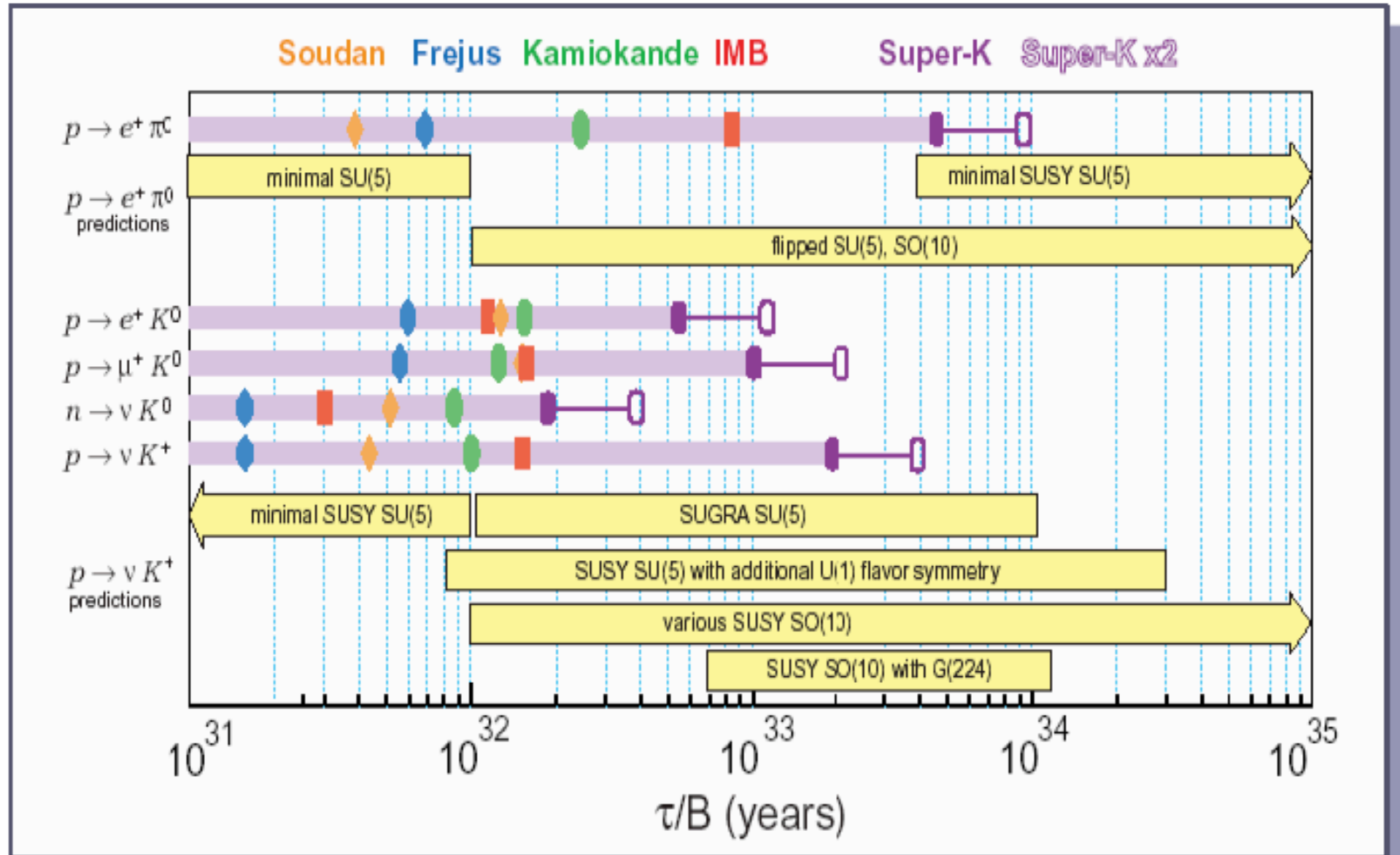
Decadimento del protone

- Nelle teorie Grandi Unificate, SU(5), SUSY, è possibile il decadimento del protone, dovuto al raggruppamento dei quark e leptoni in una simmetria più ampia.
- In SU(5) i quark e leptoni possono trasformarsi gli uni negli altri per mezzo dello scambio di *leptoquark*, bosoni pesanti X e Y.



- Poiché il tempo di decadimento scala approssimativamente con $\tau \approx M^4/m_p$, dove M è la massa del leptoquark alla scala di Planck, SU(5) suggerisce una vita media di $10^{31} - 10^{33}$ anni.
- Modelli basati sulle supersimmetrie predicono vite medie inferiori ma anche dell'ordine di 10^{35} anni.

Decadimento del protone



Violazione di CP nel mesone B

Belle experiment observes a difference in direct CP-asymmetry between charged and neutral B meson decays

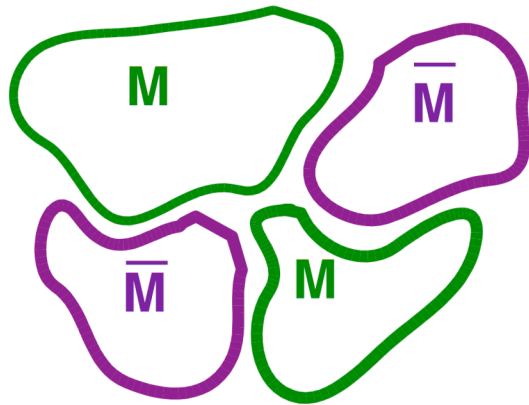
The Belle collaboration, an international research group working at the KEKB accelerator of High Energy Accelerator Research Organization (KEK) in Japan, observed a difference between direct charge-parity (CP) asymmetries for charged and neutral B meson decays into a kaon and a pion. Although it is susceptible to strong interaction effects, this difference could be an indication of a new source of CP violation that is needed to explain the matter-dominated Universe. The Belle result has been accepted for publication by Nature; this is the first time that experimental results from a B factory have been published in Nature.

Equal amounts of matter and antimatter were expected to be produced after the Big Bang, but our Universe is clearly matter-dominated. One of the prerequisites to explain the absence of antimatter is the violation of CP symmetry, a difference in the elementary properties of matter and antimatter. So far CP violation has been established only in the K^0 and B^0 meson systems, with larger effects in the latter. However, experimental results are still consistent with the mechanism proposed by Kobayashi and Masakawa, which has a unique source of CP violation that is known to be too small to explain the elimination of antimatter.

Since the effect of CP violation is very small, large quantities of data are needed to search for CP violation. In the early 21st century two experiments were dedicated to this purpose: the Belle experiment at KEK and the BaBar experiment at the Stanford Linear Accelerator Center in the USA. In 535 million $B\bar{B}$ pairs, Belle observes 2241 ± 57 $K^+ \pi^-$ and 1856 ± 52 $K^- \pi^+$ signal events. A clear height difference can be seen in Figs.1(a) and 1(b), a signature of CP violation indicating that the B^0 meson has a higher decay rate to $K \pi$. With $1600 \pm 57/-55$ π^0 signal events, more $K^- \pi^0$ signal events are observed, which is also visible as a height difference in Figs.1(c) and 1(d). However, this height deviation in the charged B sample is the opposite of that in Figs.1(a) and 1(b), suggesting different CP violation effects in charged and neutral B mesons. Our result is consistent with the previous measurements from Belle and BaBar but is more precise.

Quanta antimateria esiste nell'”universo”?
Modelli di “antibariogenesi” ?

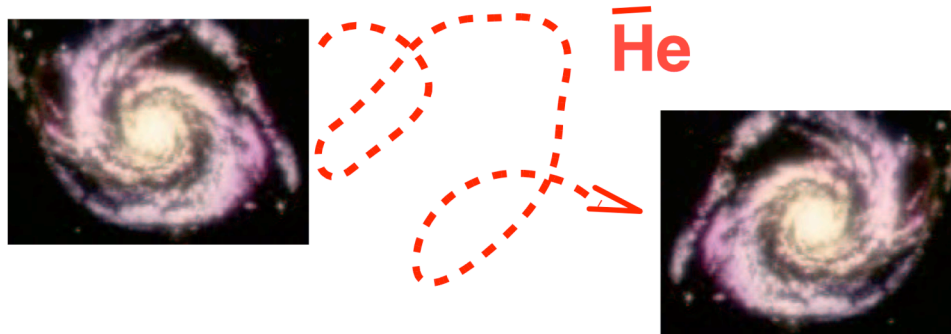
L'universo è simmetrico in materia-antimateria?



L'assenza di radiazione di
annichilazione $p + \bar{p} \rightarrow \gamma + \gamma$
nei cluster di galassie di dimensioni
tipiche $d \approx 20$ Mpc
indica che i cluster sono gli oggetti di
dimensioni più grandi che non
possono contenere quantità
significative di antimateria

Trasporto antimateria

Il campo magnetico intergalattico e gli effetti del vento magnetico introducono incertezze sul calcolo della propagazione di antimateria.



rigidità: $R = p_{\perp}/Ze$

raggio di curvatura
 $r = p_{\perp}/ZeB = R/B$

L'osservazione di antinuclei con grande *rigidità* è più promettente, perché ci potrebbe essere un cut-off magnetico.

Come rivelare l'antimateria

apparato sperimentale:

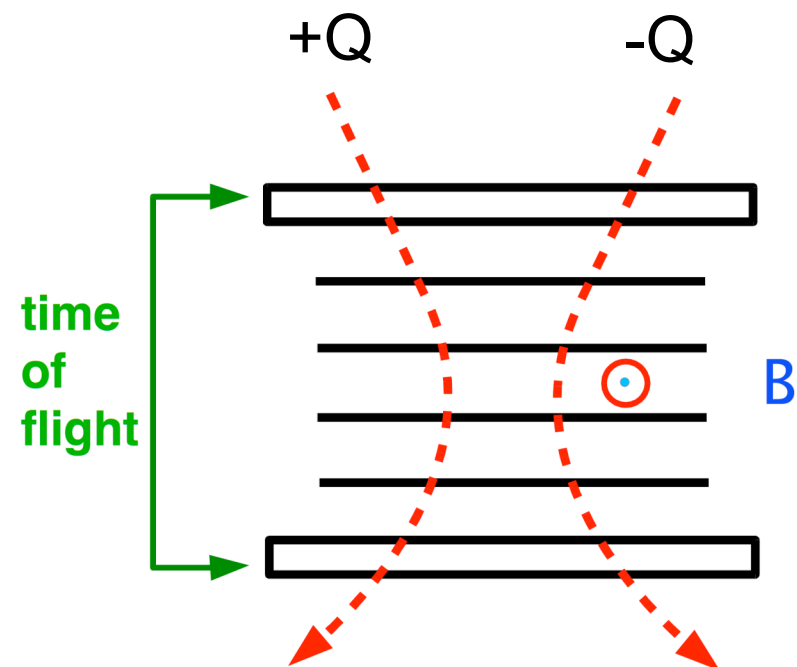
1. campo magnetico B
2. tracciatore
3. tempo di volo

$p = m\gamma v$ dal raggio di curvatura

$v = d/\Delta t$ dal tempo di volo

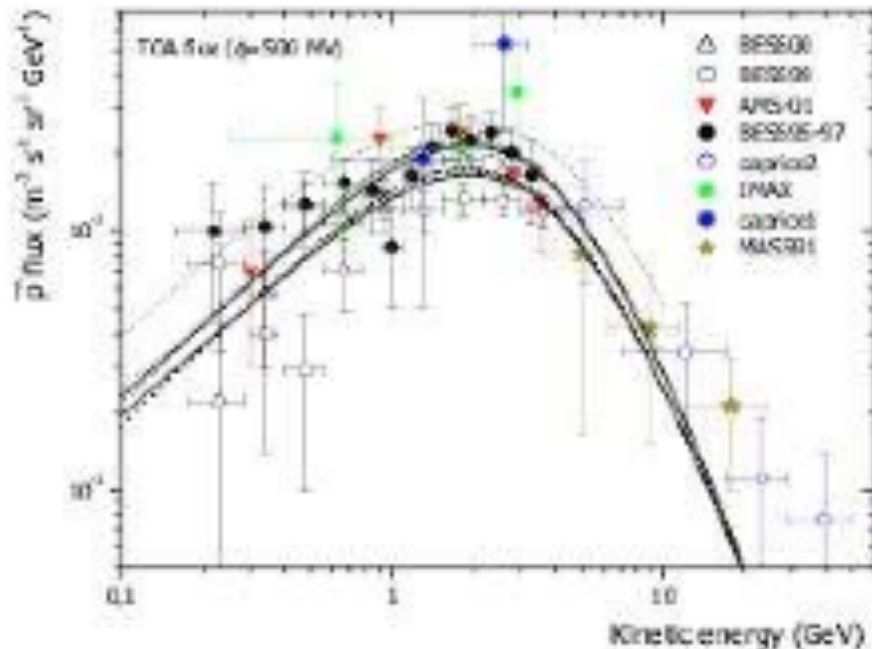
Q da dE/dx , ionizzazione

$\pm Q$ da direzione della curvatura



$m \pm Q$ identificano particella
o antiparticella

CALCOLO DEL FONDO



Antinuclei sono prodotti nelle interazioni dei RC con la materia interstellare.

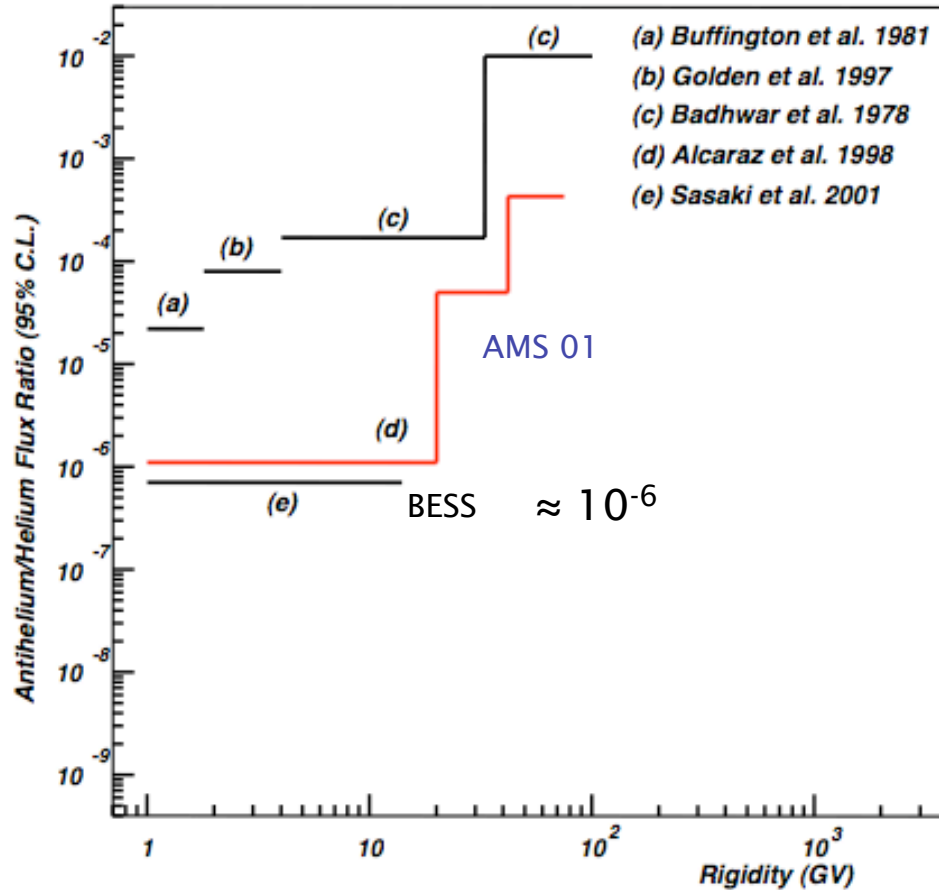
Calcolo antiprotoni: Duperray et al. (astro-ph/0503544)

Gli antiprotoni non sono un buon segnale della presenza di antimateria primordiale.

Nel caso di antielio il rapporto è

$$(\bar{\text{He}}/\text{He})_{\text{fondo}} \approx 10^{-12}$$

Limiti attuali



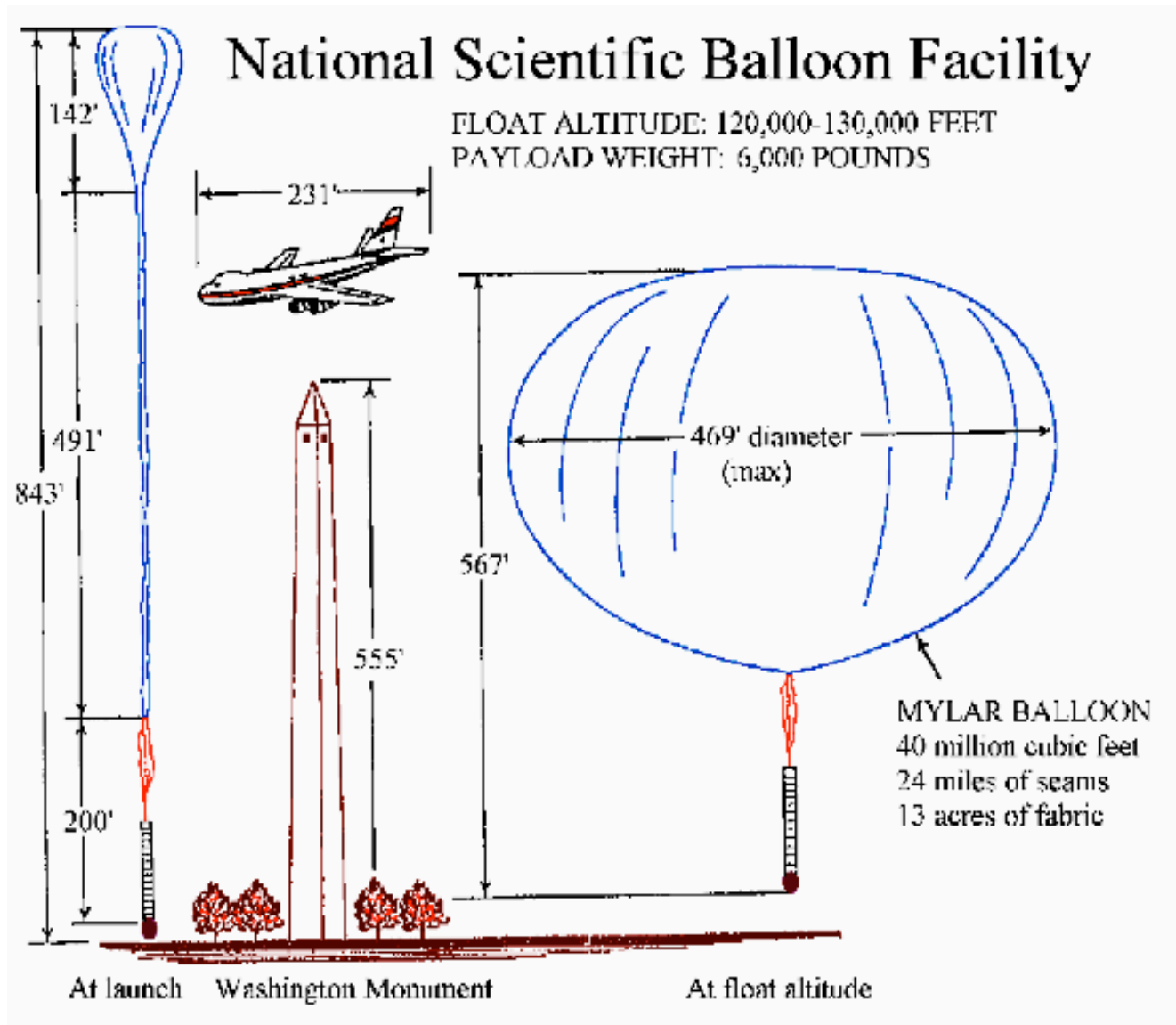
Sakharov (2001) predice
 $n(\bar{\text{He}})/n(\text{He}) \approx 10^{-6} - 10^{-8}$

$$\Rightarrow \boxed{\pm Q \quad m}$$

apparato sperimentale
ideale

- grande BL^2
- direzione “alto-basso”
- rivelatori con spessori minimi
- tracce con punti ridondanti

ESPERIMENTI SU PALLONE





BESS



The current incarnation of the BESS instrument, BESS-Polar, is similar in design to previous BESS instruments, but is completely new with an ultra-thin magnet developed at the High Energy Accelerator Research Organization (KEK) and configured to minimize the amount of material in the cosmic ray beam, so as to allow the lowest energy measurements of antiprotons.

BESS-Polar has the largest geometry factor of any balloon-borne magnet spectrometer currently flying, and is ideally suited to statistics-limited studies of $Z=1$ and $Z=2$ components - identifying antiprotons, and searching for antihelium nuclei in the cosmic radiation. BESS-Polar has a geometrical acceptance of $0.3 \text{ m}^2\text{-sr}$, an aerogel Cherenkov counter with index of refraction $n=1.02$ and a time-of-flight system with 150 ps resolution, capable of identifying antiprotons over the energy range from 100 MeV to 4.2 GeV .

BESS-Polar is scheduled to make its maiden flight from McMurdo, Antarctica in December 2004. A second flight at the time of minimum solar activity is planned for 2007. The extended data-taking time of long duration flights, the increased event efficiency of the BESS-Polar configuration and the low geomagnetic cutoff should together allow an improvement factor of more than 20 over existing low-energy antiproton data.

BESS

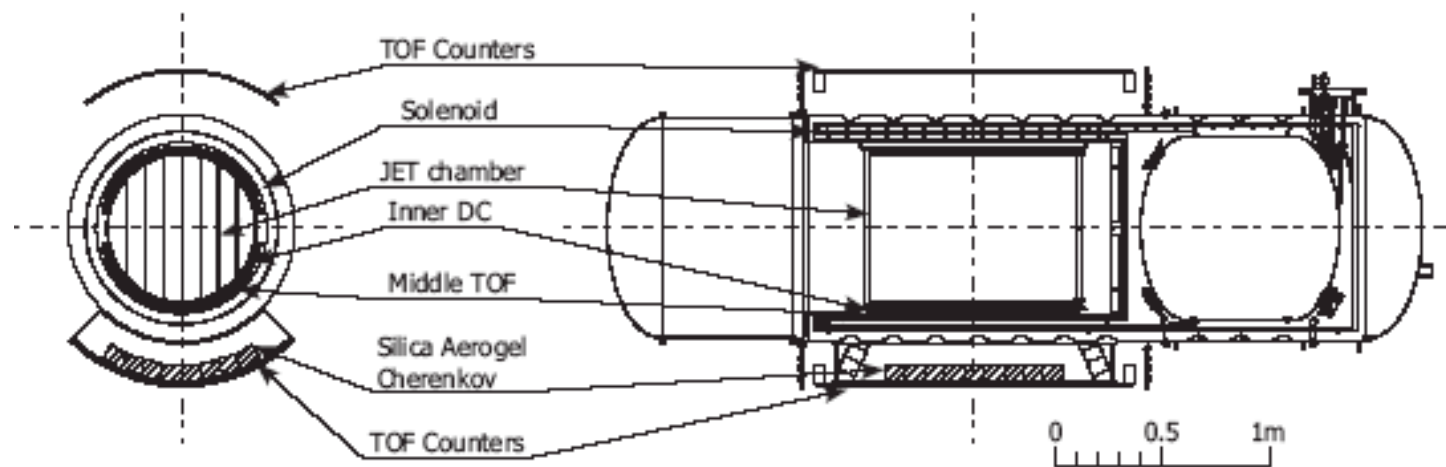


Fig. 1. Cross-sectional views of the BESS-Polar spectrometer

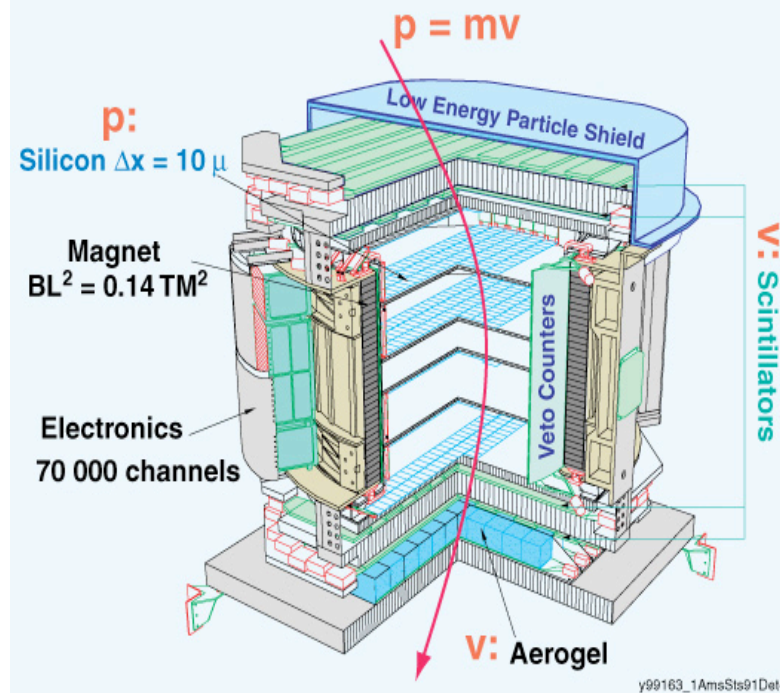
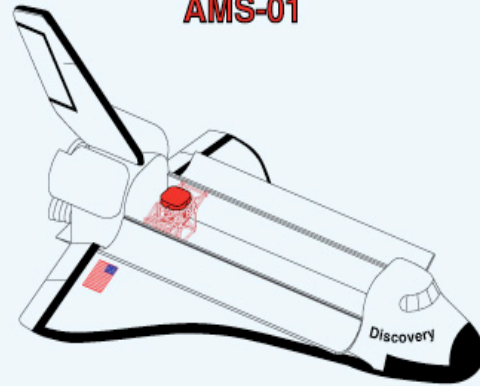
Table I. BESS-Polar spectrometer design parameters.

Geometrical acceptance	0.3 m ² sr
Flight duration	10 ~ 20 days
Energy range for p-bar (@TOA)	0.1 ~ 4.2 GeV
Magnetic field	0.8(~ 1) T
Distance between TOF counters	1.47 m
Diameter of Central tracker (JET/IDC)	0.75 m
Maximum detectable rigidity	150 GV
Power consumption	600 W
Material in upper-half detector wall	4.5 g/cm ²
Over-all payload size ($x/y/z$)	1.5/1.5/4 m
Weight	1.5 ton

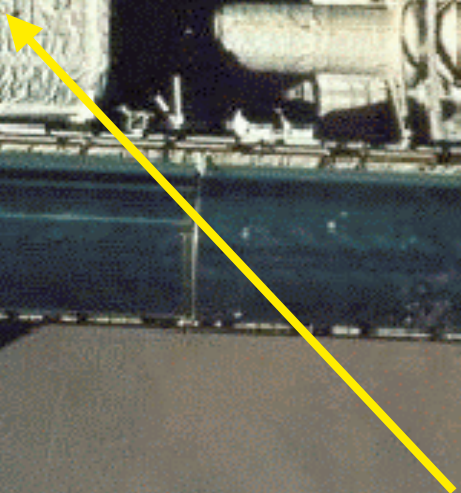
AMS-01: volo STS-91/ Discovery

First flight, STS-91, 2 June 1998 (10 days)

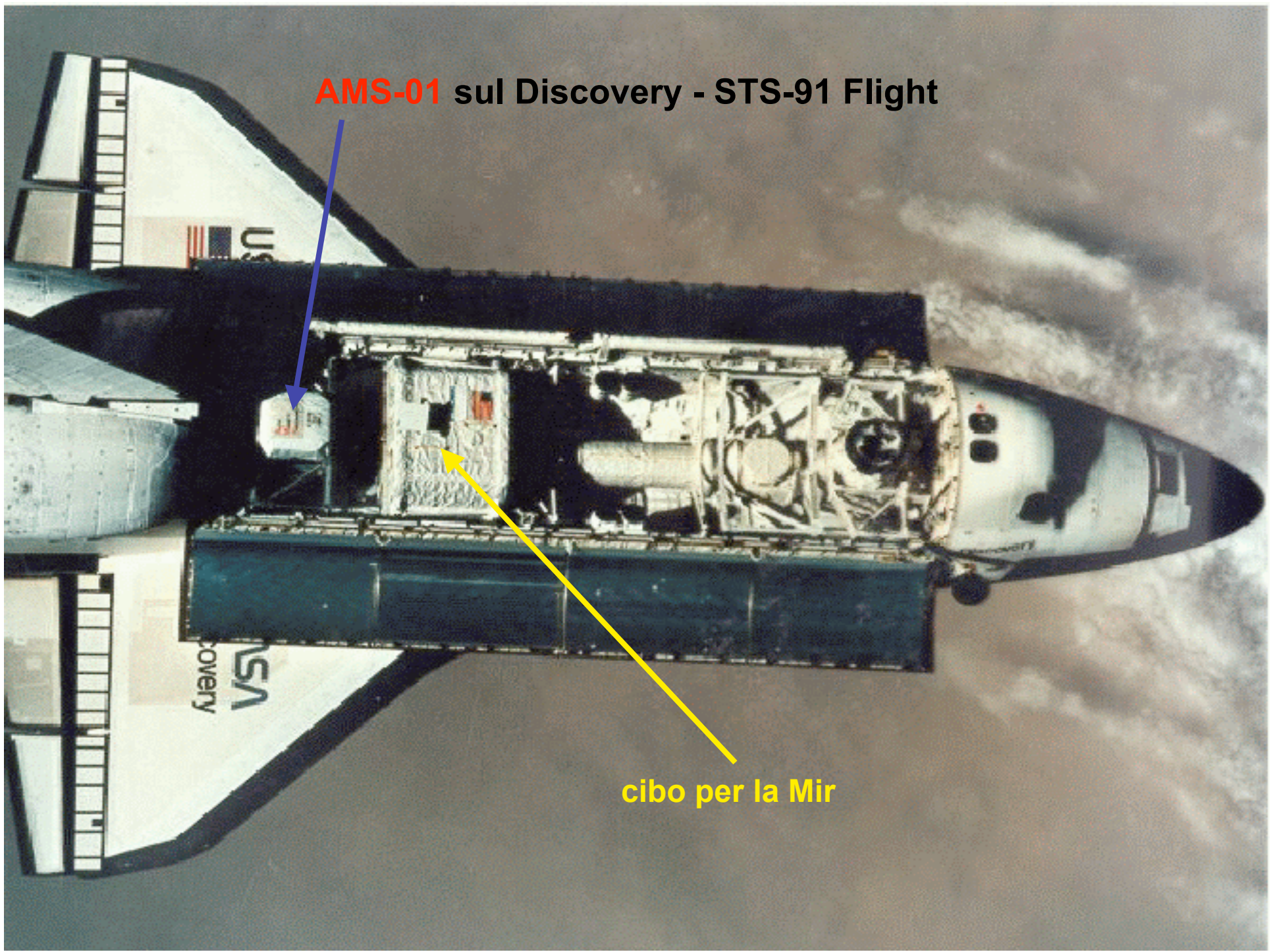
AMS-01



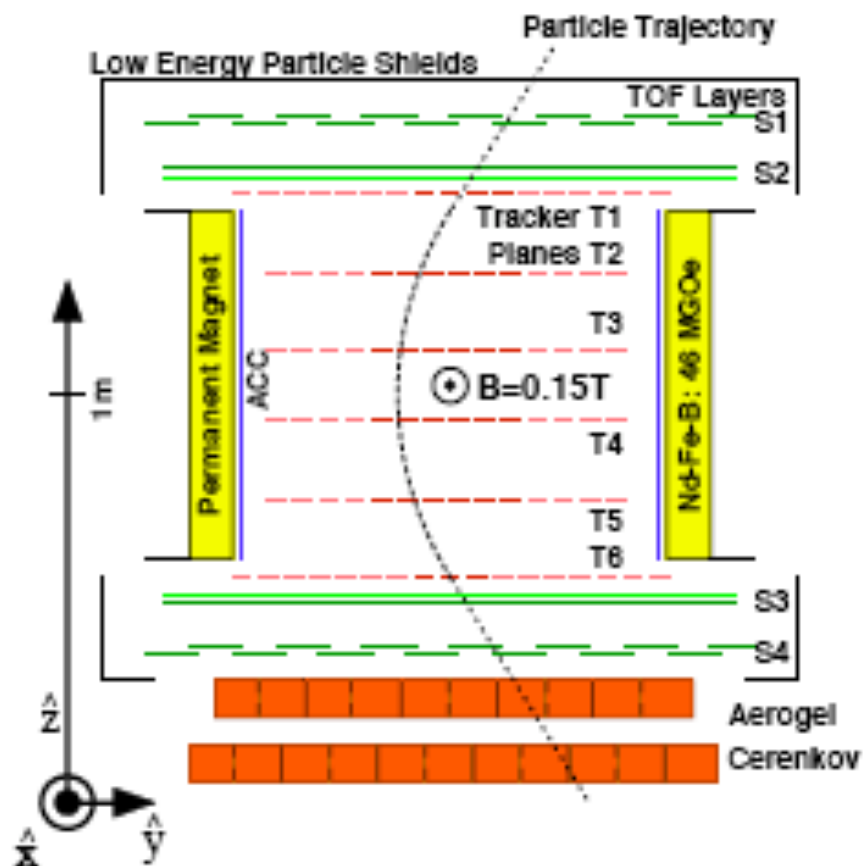
AMS-01 sul Discovery - STS-91 Flight



cibo per la Mir

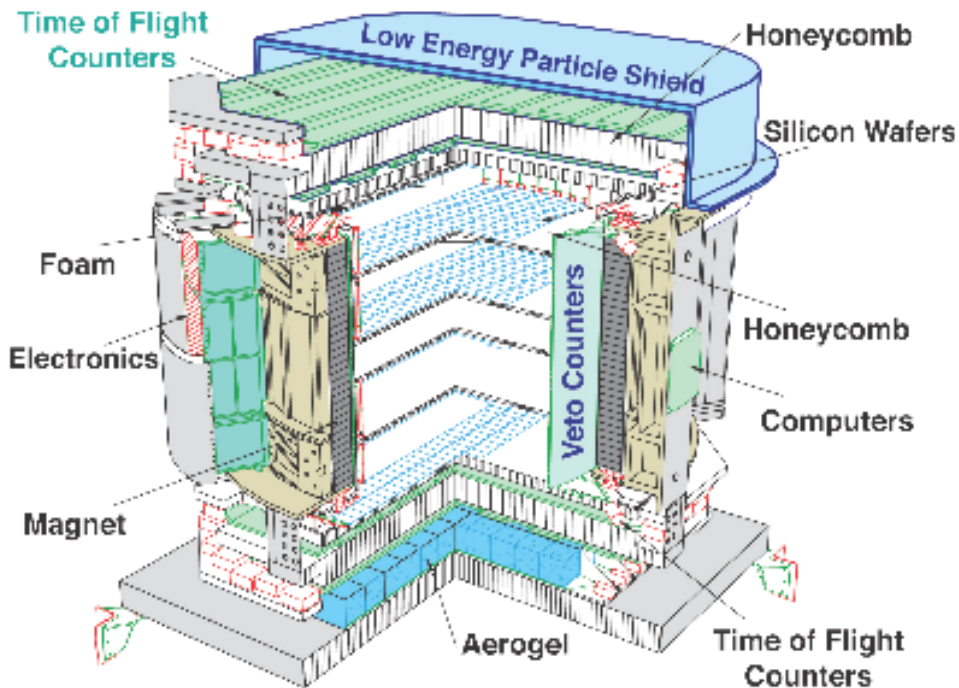


AMS-01



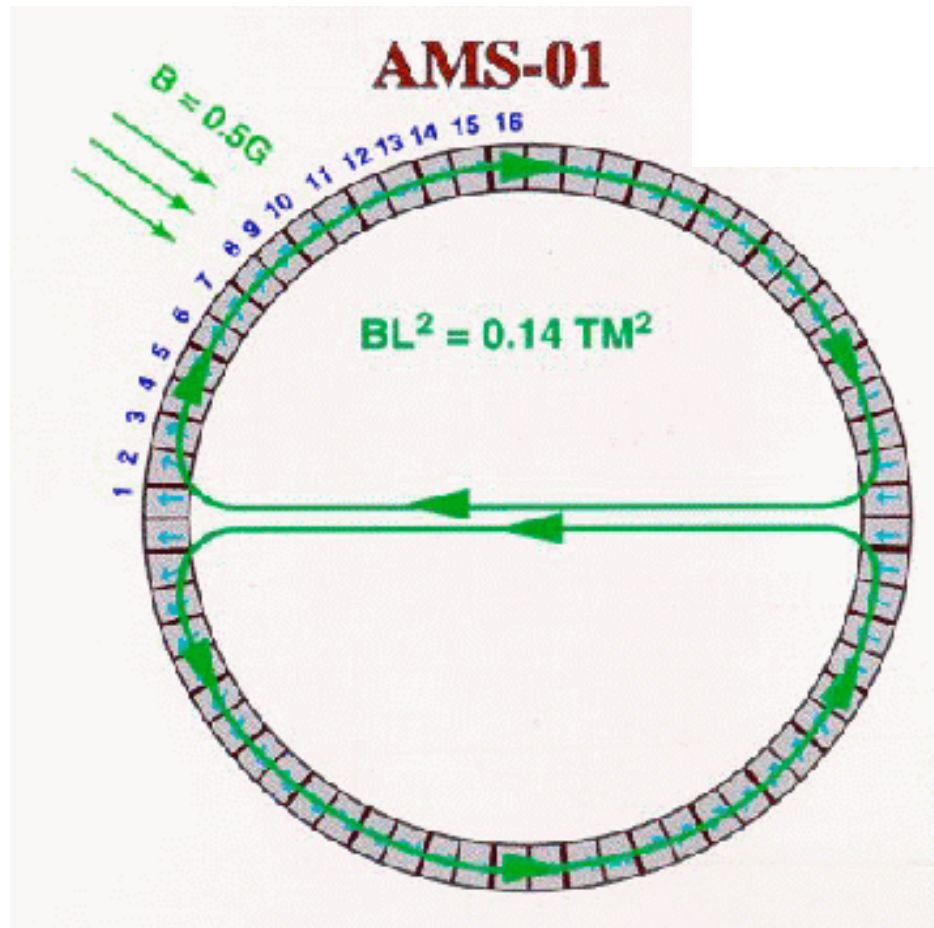
- STS91 2-11 June 1998
Shuttle Discovery
- Mean altitude 370 km
- 90 min orbit inclined at 51.7°
- Trigger-rate 100-700 Hz
- Recorded 10^8 events in 100 h

AMS-01



- magnete permanente, $BL^2 = 0.14 \text{ Tm}^2$
- tracciatore μ strip silicio, $\Delta x \approx 10 \mu\text{m}$
 $p/Ze, dE/dx, \pm Q$
- 4 piani scintillatori tempo di volo, $\Delta t \approx 100 \text{ ps}$
 v, Q
- Cerenkov aerogel
 v/c

AMS-01: Magnete permanente



diametro $d = 1\text{ m}$

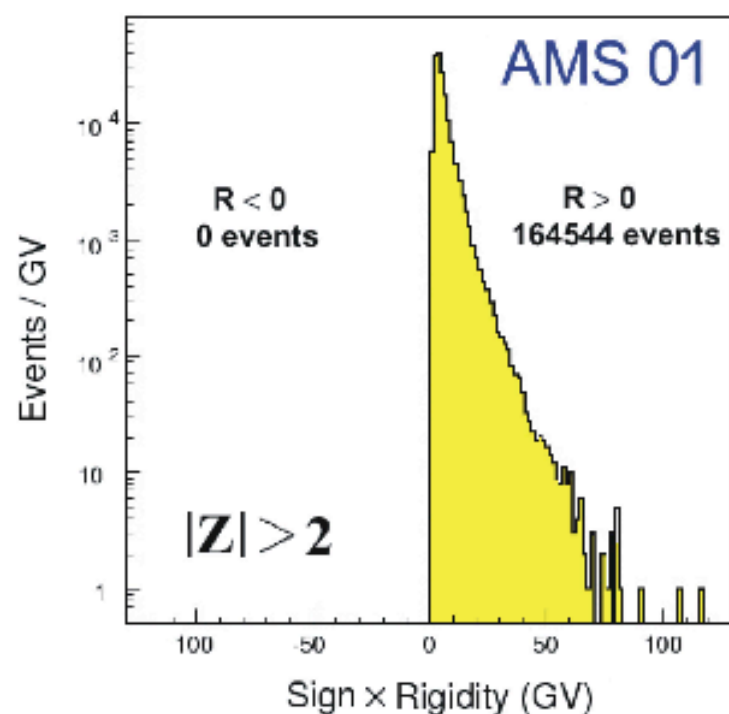
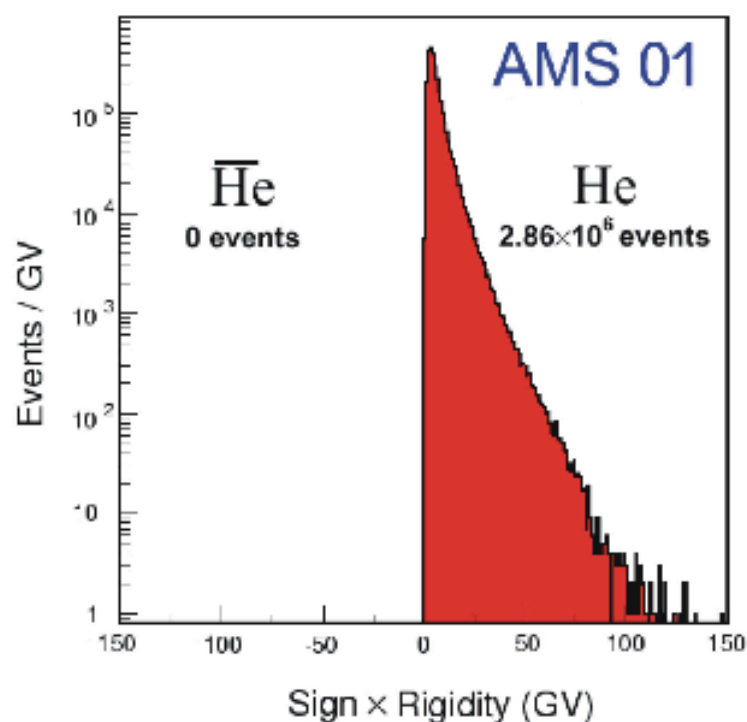
$h \approx 1\text{ m}$

momento di dipolo ≈ 0

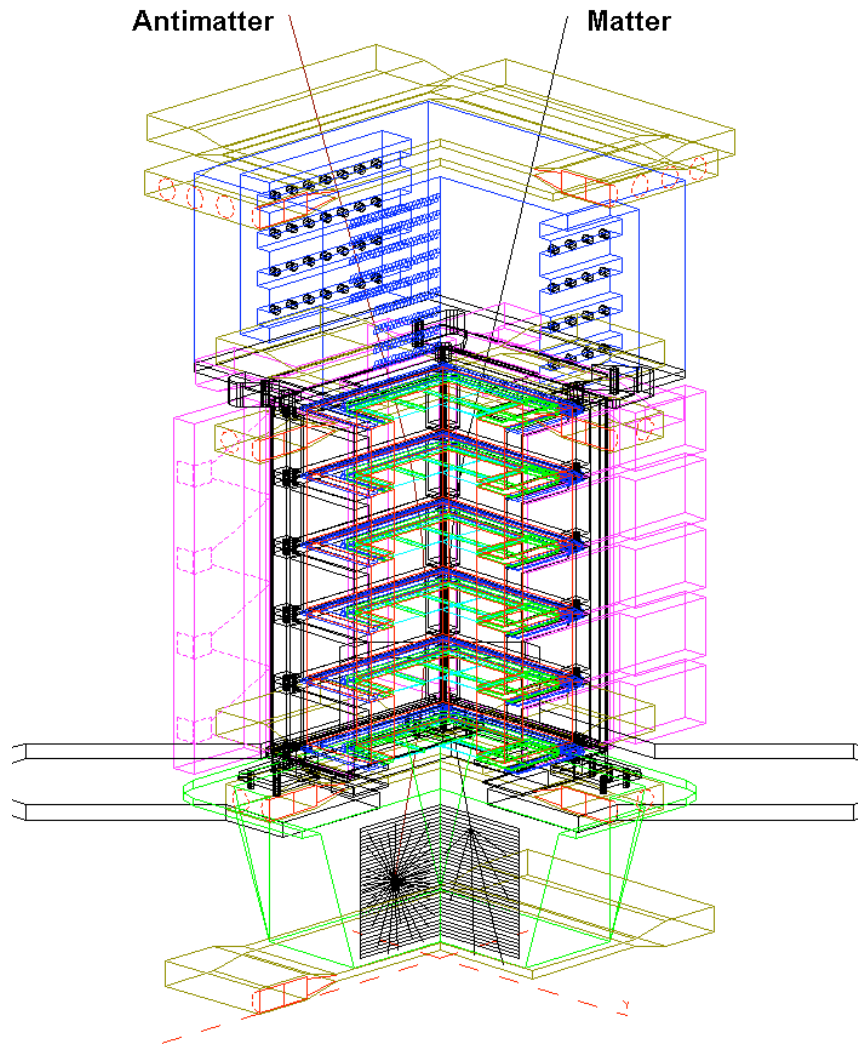
campo disperso $< 60\text{ G}$

Search for Antimatter

AMS-01 10 day precursor flight



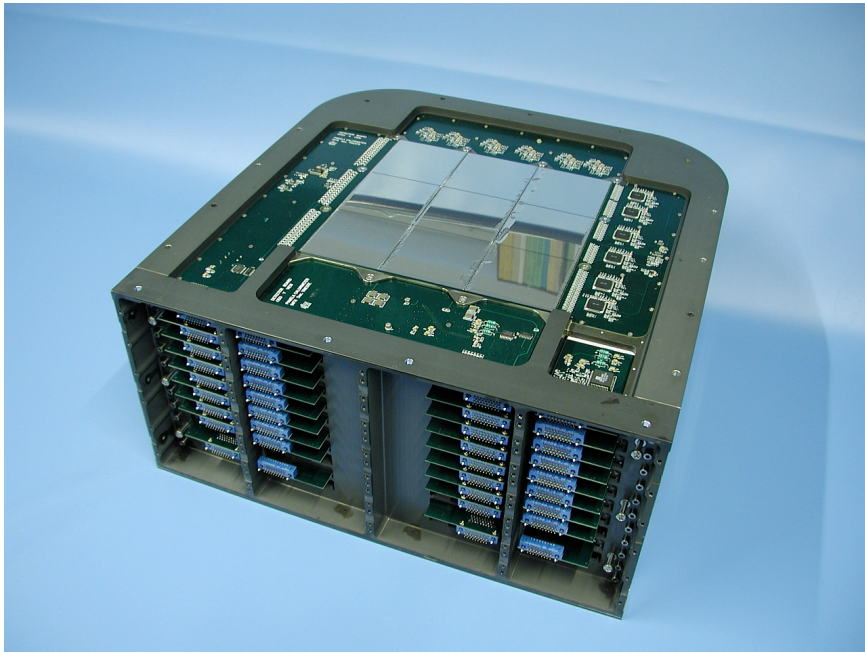
PAMELA



The PAMELA experiment will be installed on the up-ward side of the Resurs-DK1 satellite and will be launched to september 2005. The satellite will orbit the Earth along an elliptical orbit with an average altitude of 500 Km and an inclination of 70.4 deg. The experiment is expected to be operating for at least 3 years. In this period there will be collected:

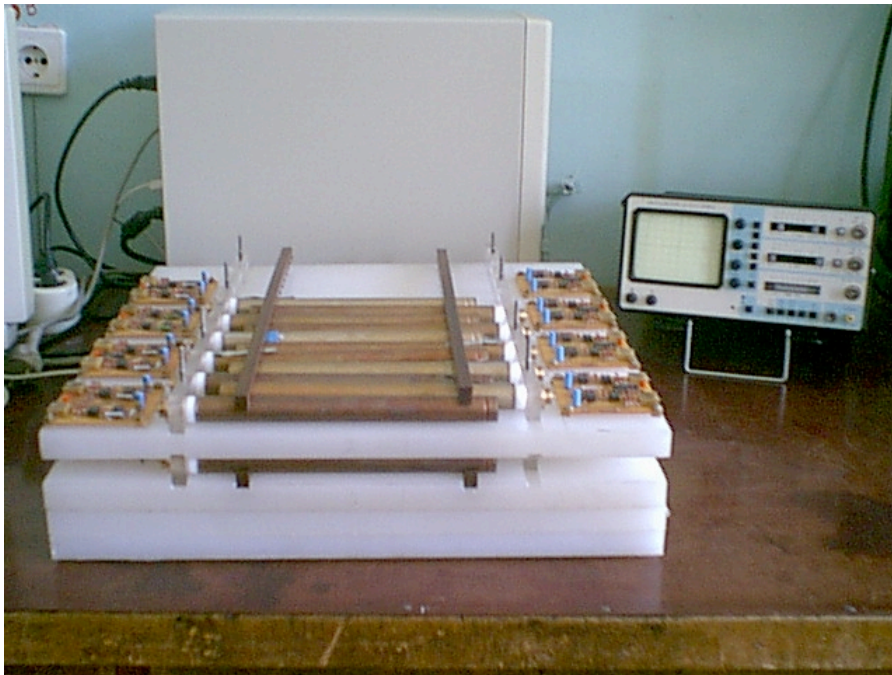
<i>Particle</i>	<i>Number</i>	<i>Energy Range</i>
protons	3×10^8	80 MeV-700 GeV
antiprotons	$> 3 \times 10^4$	80 MeV-190 GeV
electrons	6×10^6	50 MeV-2 TeV
positrons	$> 3 \times 10^5$	50 MeV-270 GeV
He nuclei	4×10^7	up to 700 GeV/n
Be nuclei	4×10^4	up to 700 GeV/n
C nuclei	4×10^5	up to 700 GeV/n
antinuclei	$< 7 \times 10^{-8}$	up to 30 GeV/n
limit (90% c.l.)		

PAMELA- CALORIMETRO EM



- The imaging em Calorimeter has a mass of 110 Kg and is composed of 23 layers interleaving Silicon sensors for the X- and Y-coordinate and Tungsten absorbing planes, each 2.3 mm thick. The total thickness corresponds to 0.9 interaction lengths and 16 radiation lengths. Each sensitive layer contains an array of 3 x 3 ministrip Silicon sensors. The total number of channels is 4416. The main purpose of the calorimeter, besides the energy measurements of e- and e+, is the identification of antiprotons and positrons. The Rejection Power of electrons (in the antiprotons sample) and protons (in the positrons sample) is greater than 10^4 with an efficiency of 90%. The energy resolution for high energy electrons is better than 10% and the momentum resolution for 10 GeV protons is better than 10%.

PAMELA- CONT. NEUTRONI

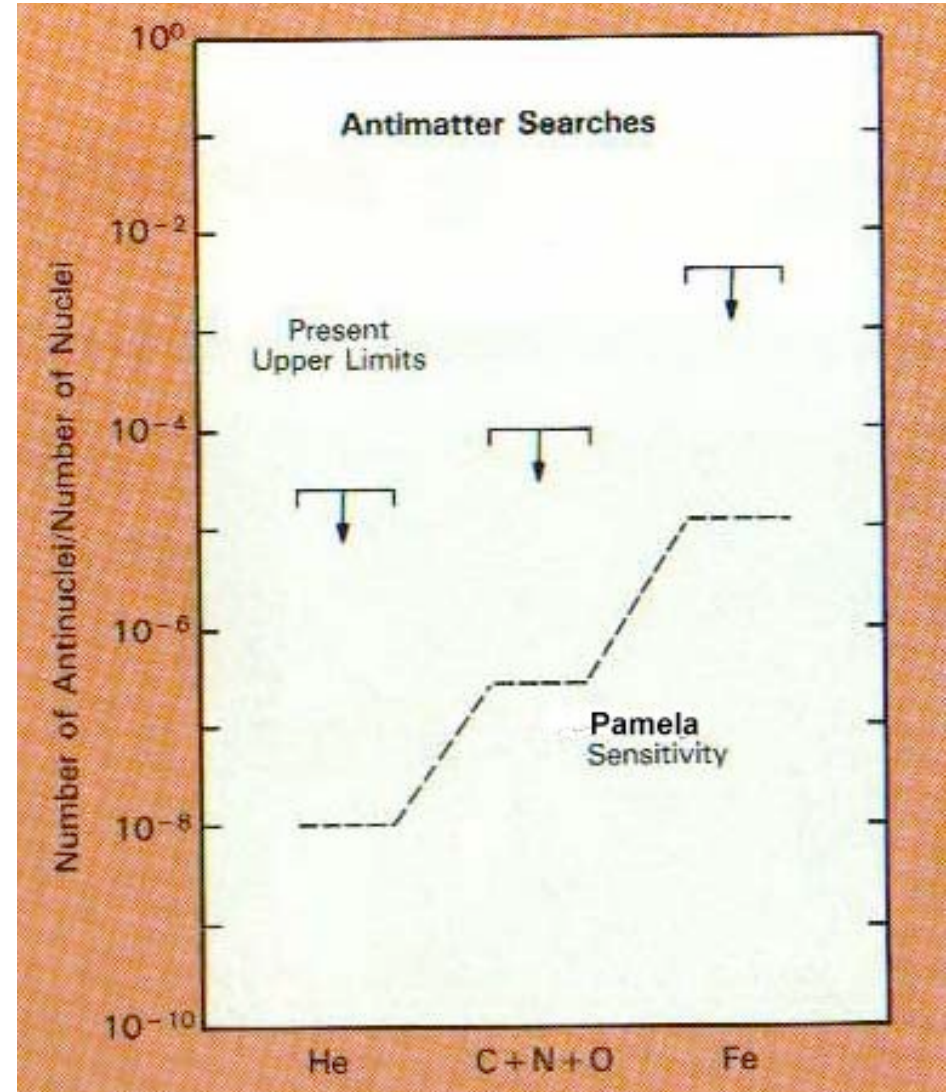
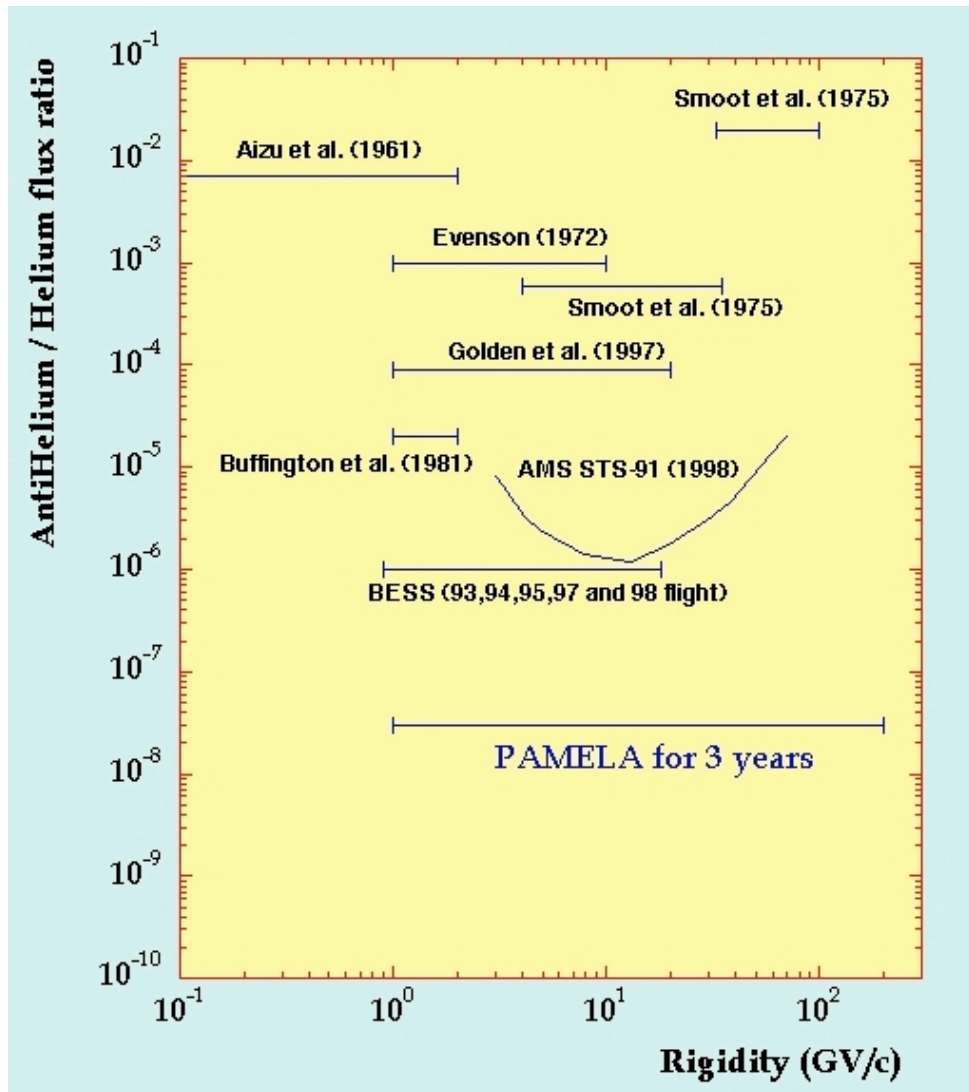


- A Neutron Detector has been added to the PAMELA instrument with the aim to expand the energy range of the recorded primary protons and electrons up to 10^{11} - 10^{13} eV.
- It consists of 36 ^3He counters enveloped by a polyethylene moderator. Since the ^3He counters are sensitive to the thermal neutrons, an efficiency of evaporated neutron detection taking into account the efficiency of thermalisation is around 10%.
- The size of the Neutron Detector is $600 \times 550 \times 150 \text{ mm}^3$, the total weight is 30 kg. The signal from the Neutron Detector is used for the selection of leptons over the background of hadrons, making use of the different neutron yield from hadron-initiated and electromagnetic showers.
- The evaporated neutron yield in the hadron-initiated cascades, indeed, is almost 20 times larger than that from electromagnetic cascades.
- Including the Neutron Detector in the PAMELA instrument allows the primary proton and electron spectra to be studied at energies above some hundreds of GeV. The Neutron Detector is capable of distinguishing primary protons and electrons at energies 10^{11} - 10^{13} eV with a rejection factor of about 10^{-4} .

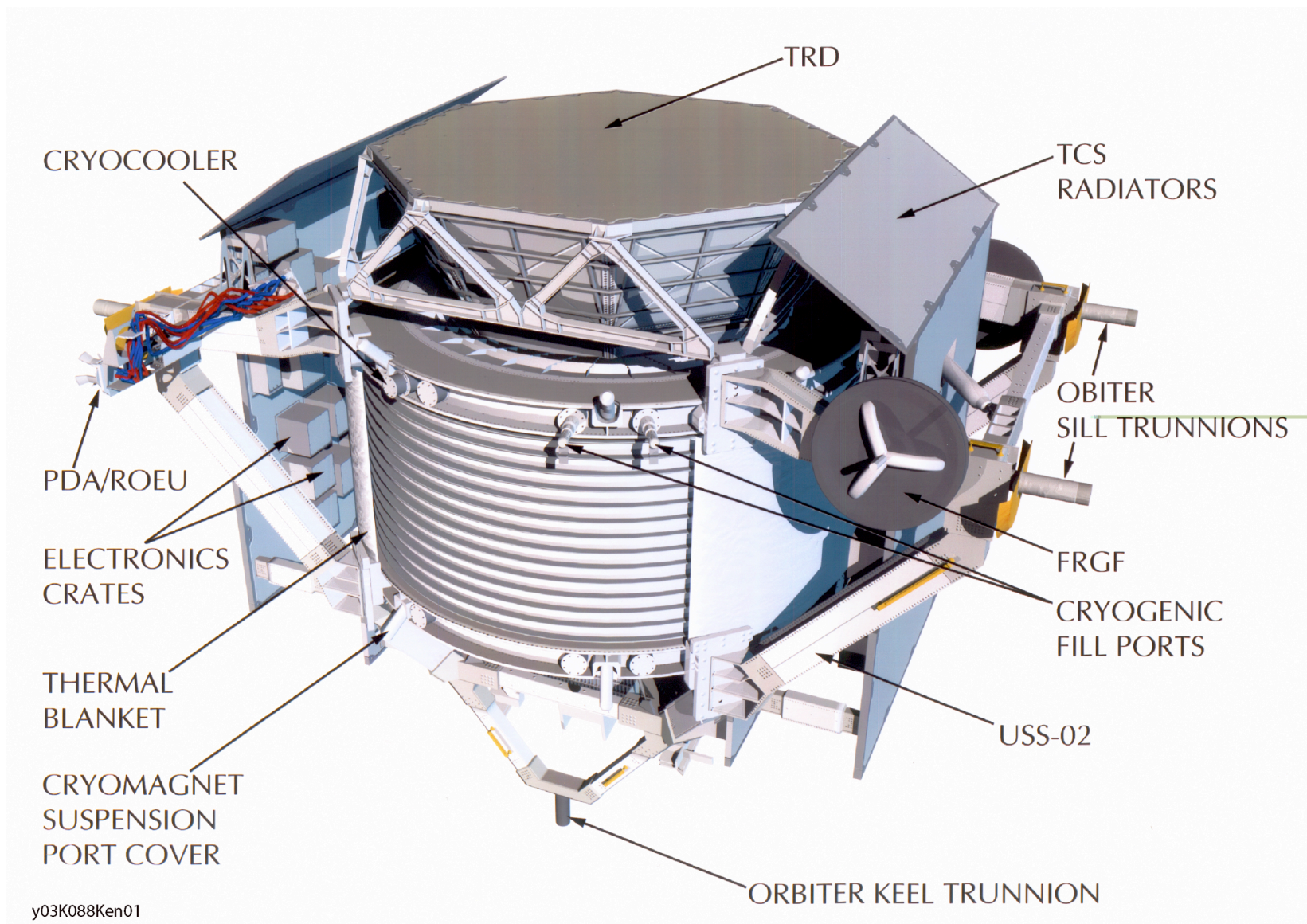
PAMELA

$\bar{\text{He}}/\text{He}$

$\bar{\text{N}}/\text{N}$

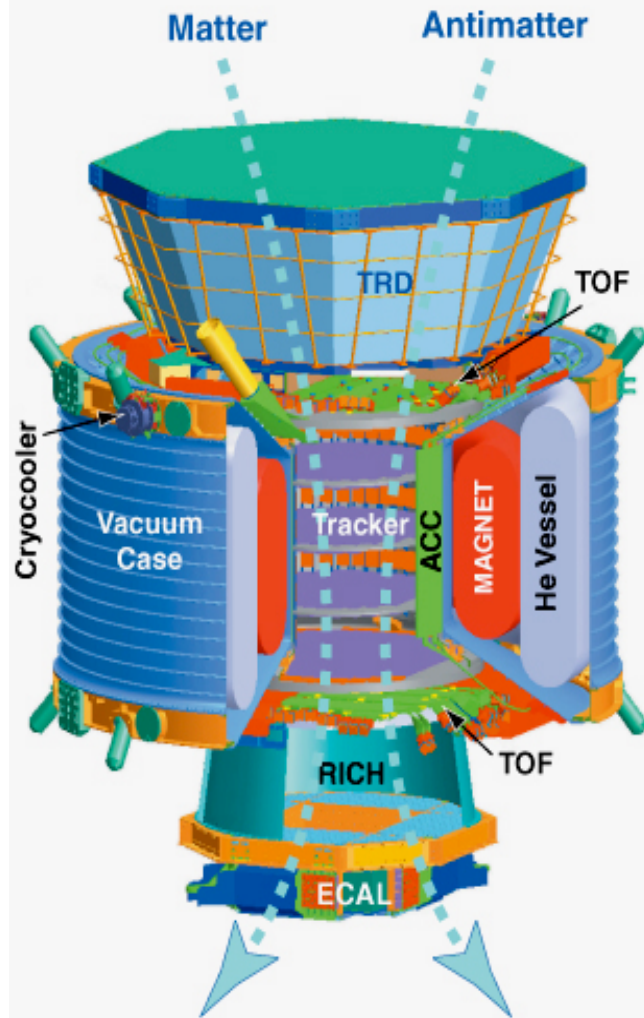


AMS-02



payload 7 ton; 2200 W; ≥ 3 anni sulla ISS

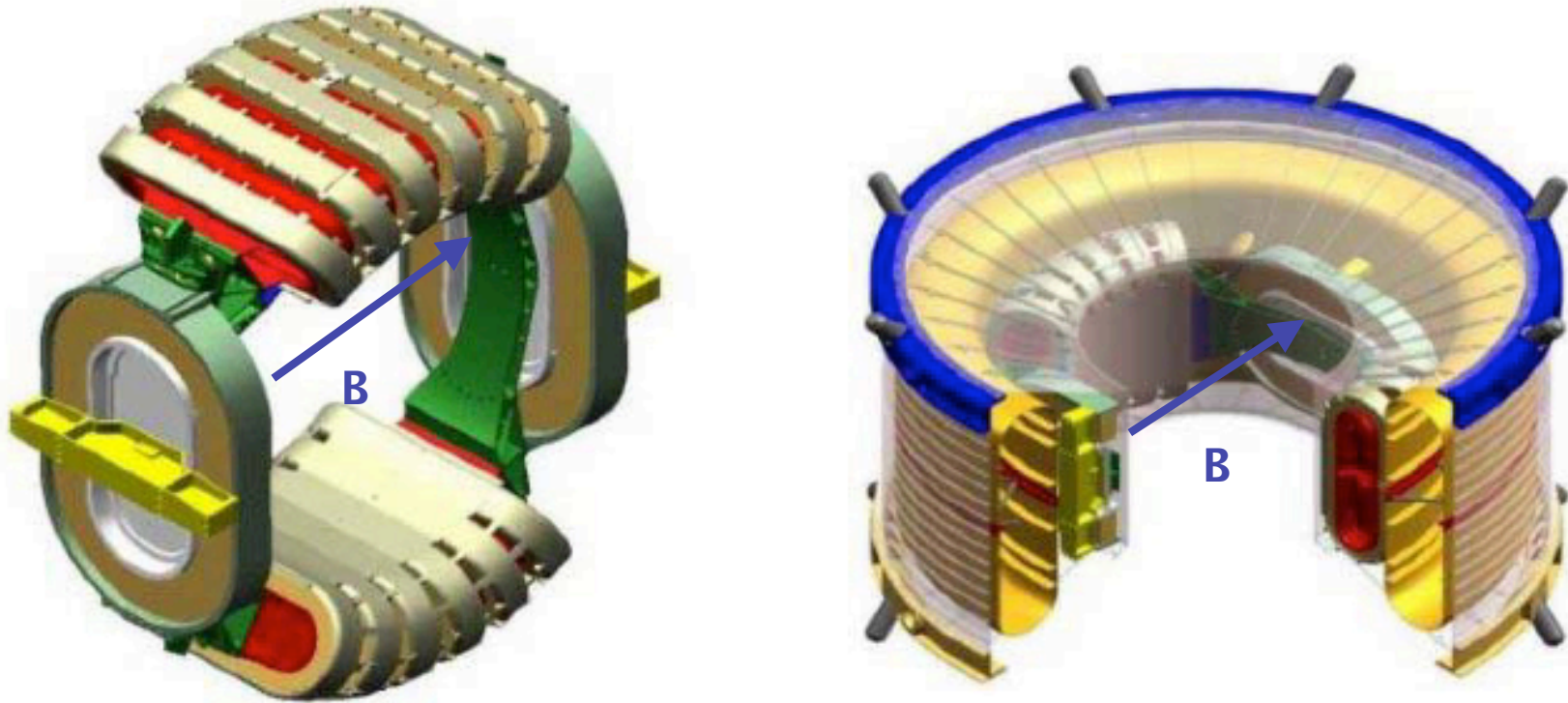
AMS: A TeV Magnetic Spectrometer in Space (3m x 3m x 3m, 7t)



300,000 channels of electronics $\Delta t = 100 \text{ ps}$, $\Delta x = 10 \mu$

0.3 TeV	e^-	e^+	P	$\bar{\text{He}}$	γ
TRD					
TOF					
Tracker					
RICH					
Calorimeter					

Magnet layout & vessel



360 Kg superfluid He
 $T = 1.8\text{K}$

No dipole field
Stray field < 500 Gauss
max current 450A

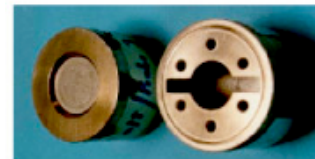
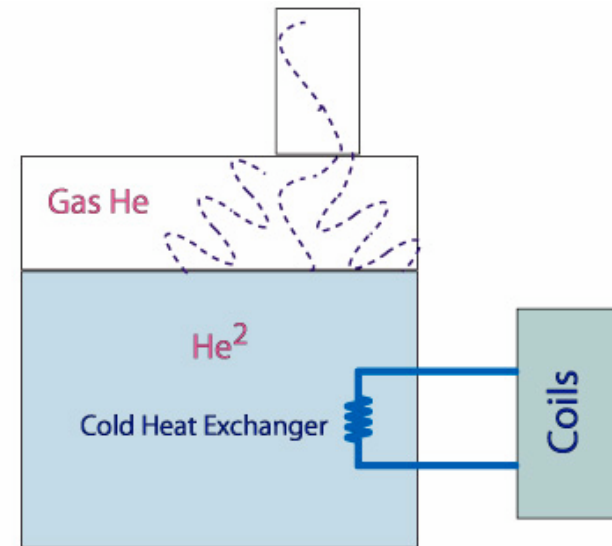
Superfluid He in space

He II:

- zero viscosity
- density > He I
- high thermal conductivity
- low thermal capacitance

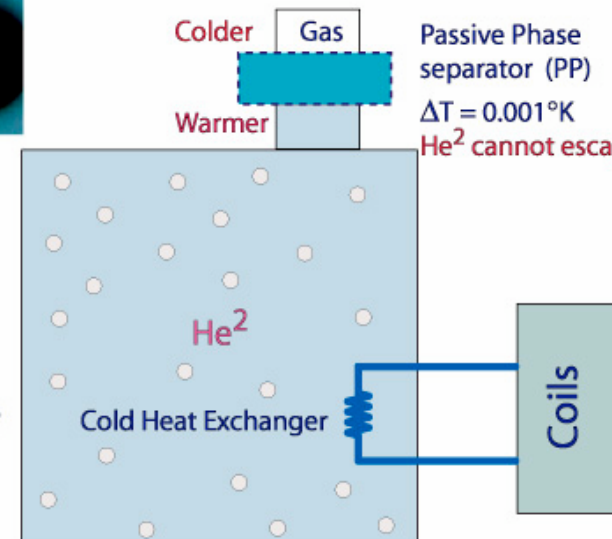
On ground

Linde



Colder Gas
Warmer
Passive Phase separator (PP)
 $\Delta T = 0.001^\circ\text{K}$
He² cannot escape.

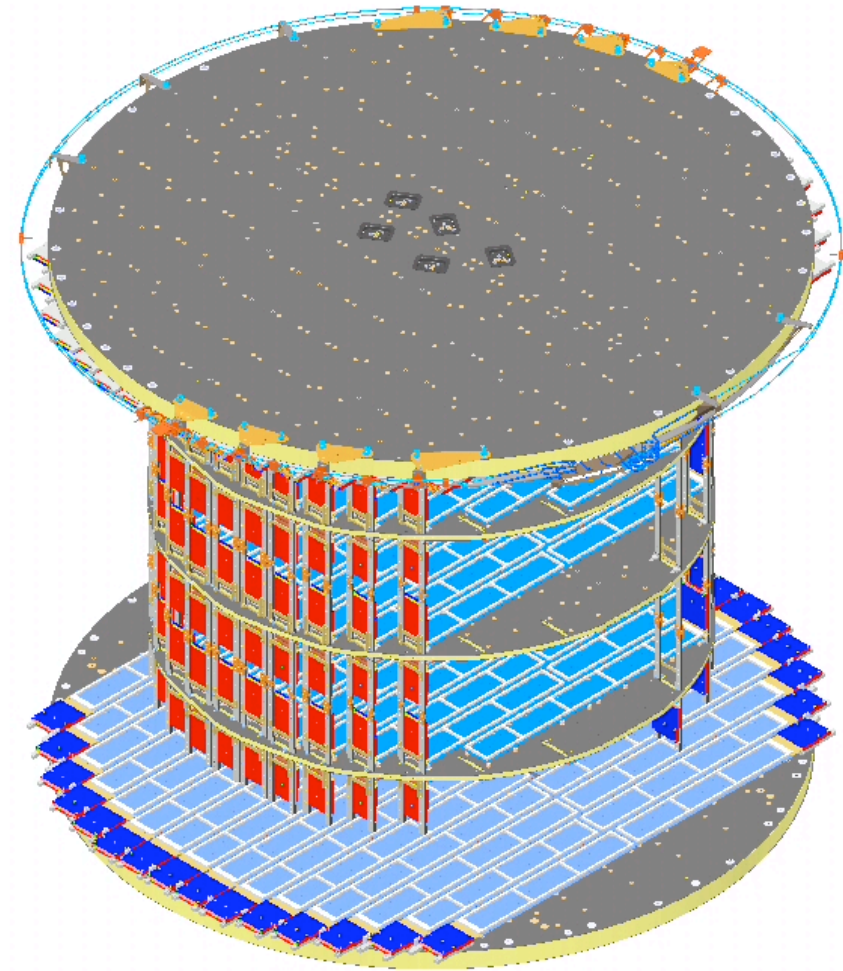
in space



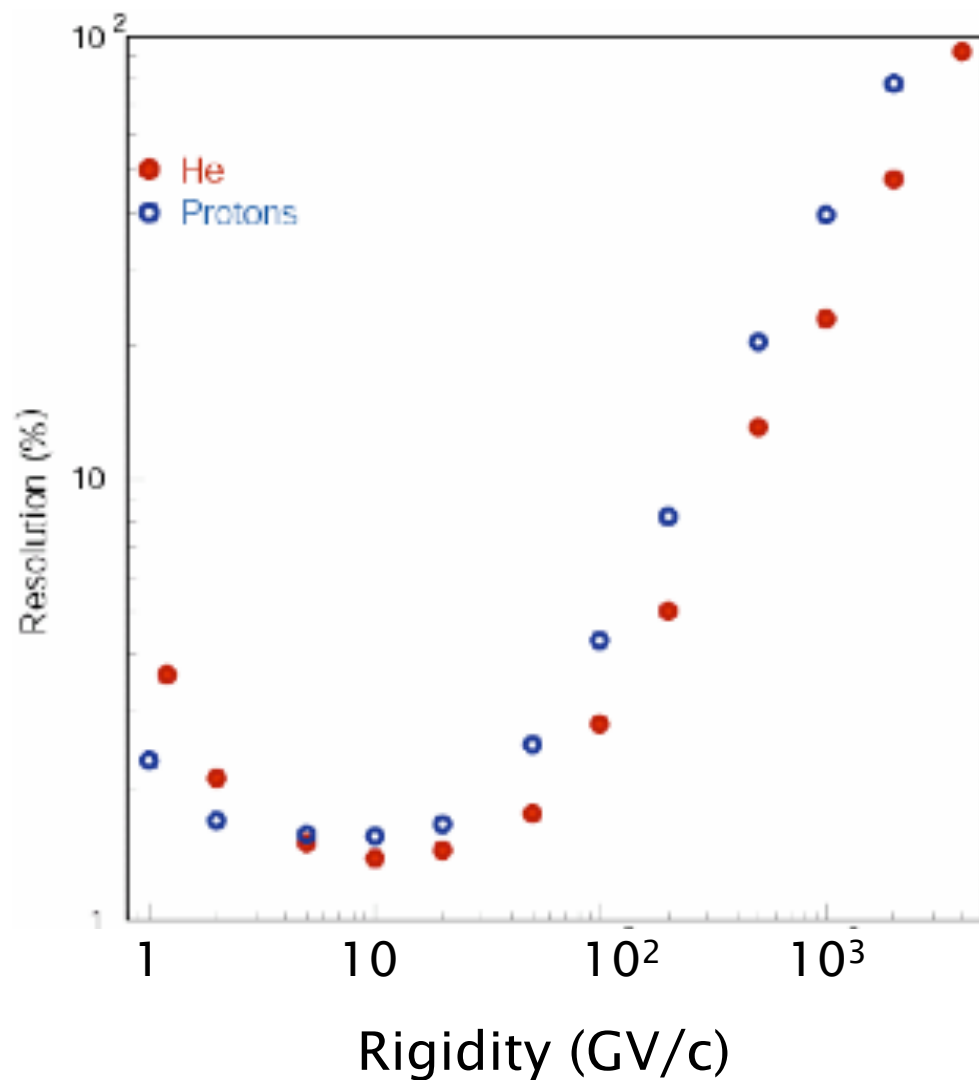
He II
fountain effect:
flows to
warmer environment

TRK layout

- 2 planes single layer at conical flanges
- 3 planes x 2 layers inside cylindrical zone
- total 8 layers with xy measurements
- material
 - sensors+hybrids 3.2% X_0
 - honeycomb 0.7% X_0
 - total 3.9% X_0

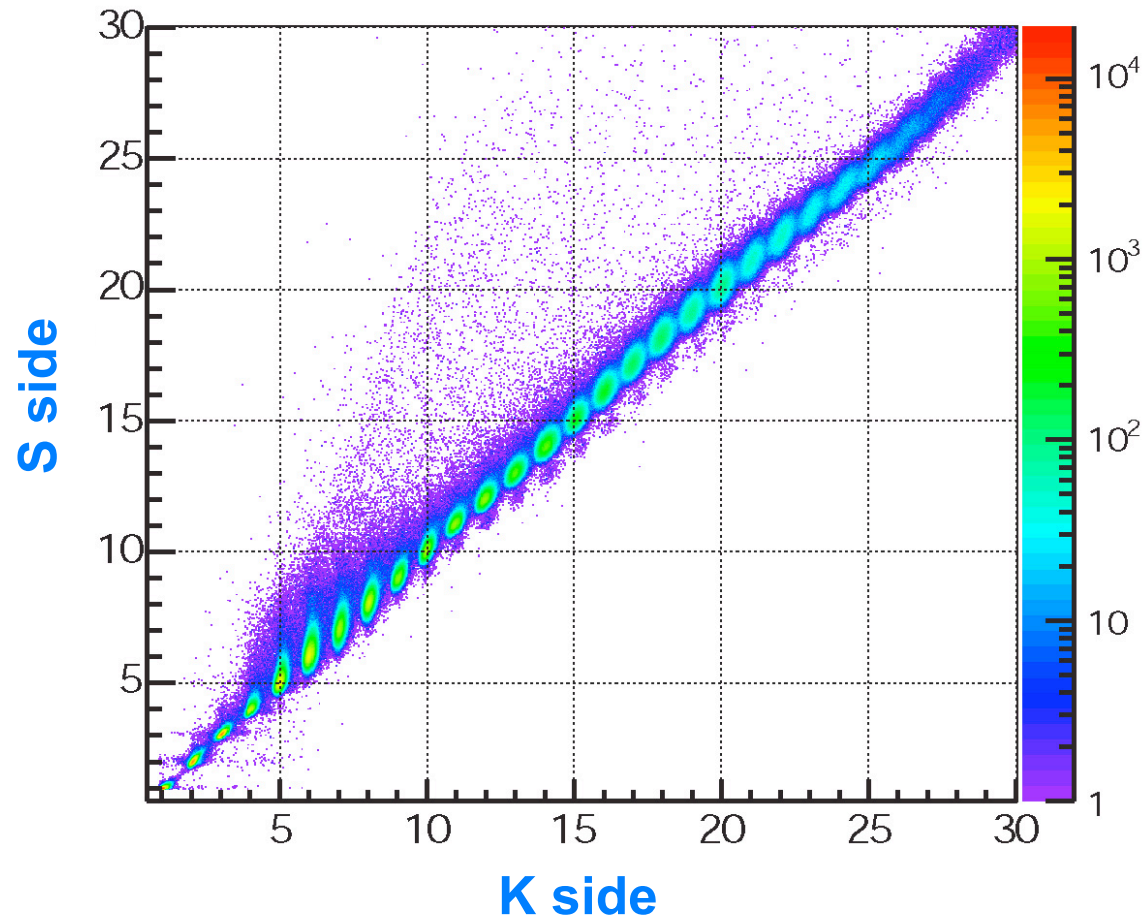


TRK rigidity resolution

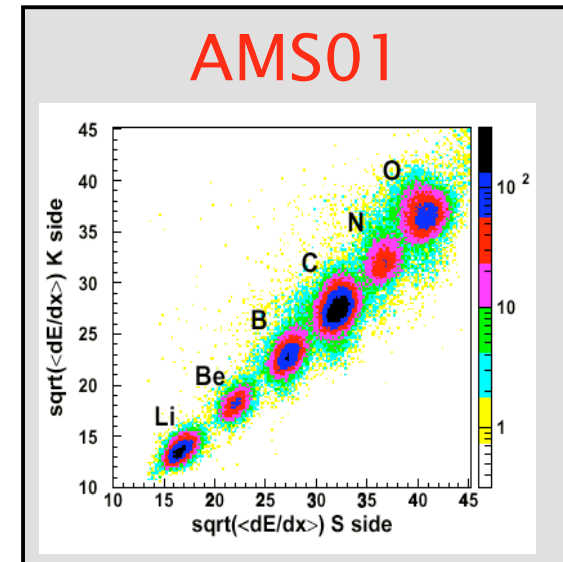


- Protons
 $\Delta p/p \approx 20\%$ @ 0.5 TV
- He
 $\Delta p/p \approx 20\%$ @ 1 TV

Charge Measurement with Silicon Tracker



Fragments from a beam at 158 GeV/c/A



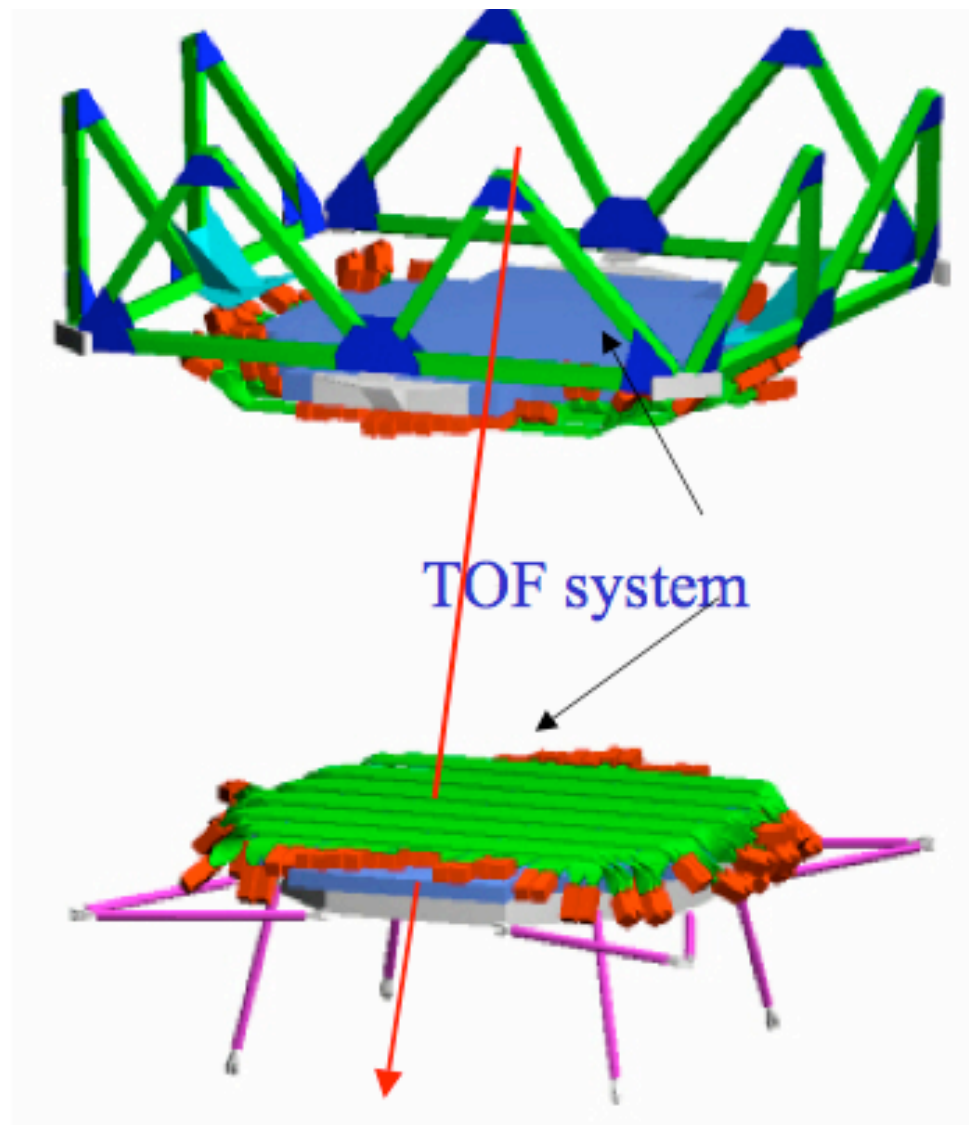
Time Of Flight

- up/down: $(t_d - t_u) > 0$

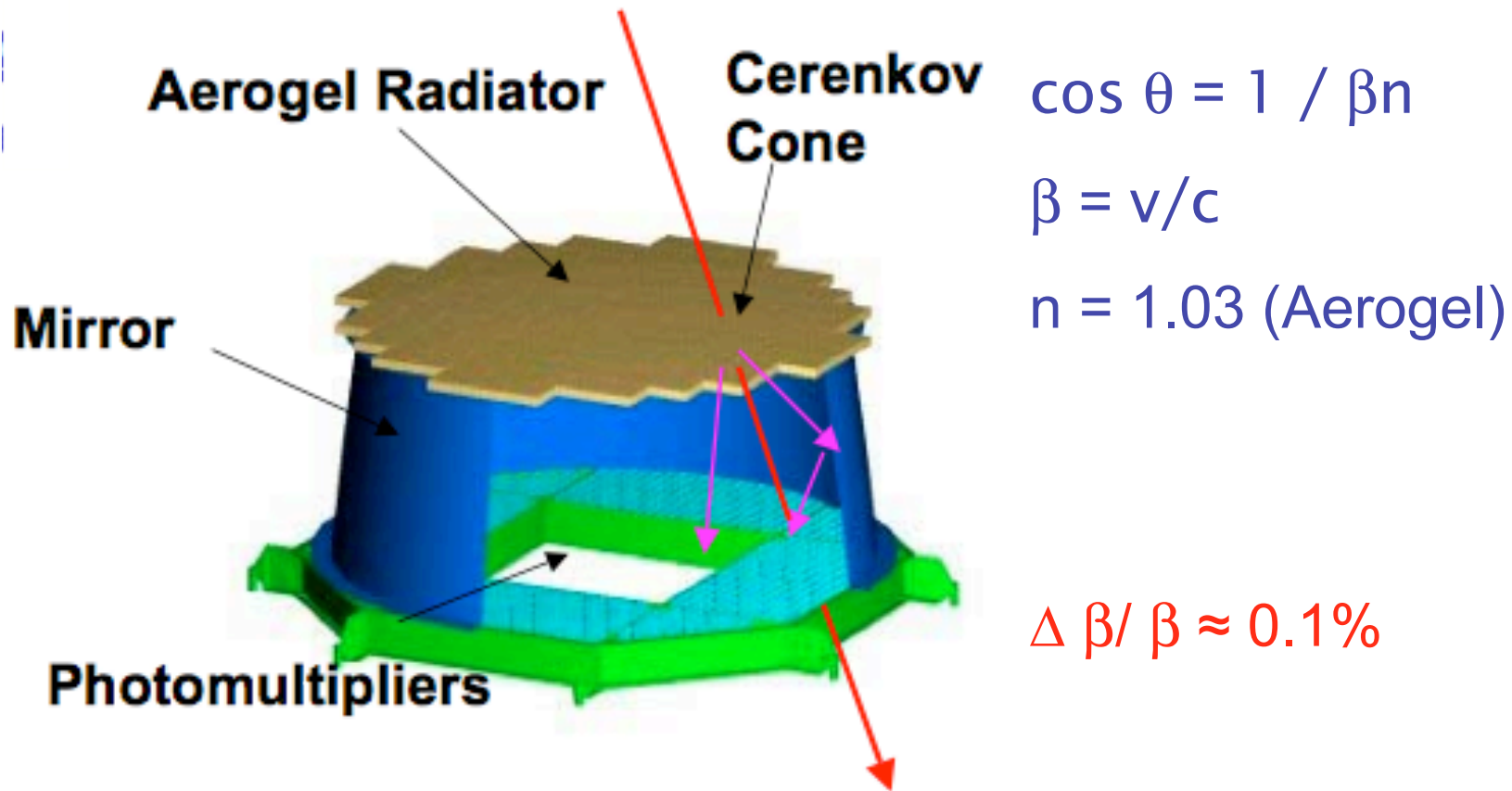
- $v = d / (t_d - t_u)$

- $Z \propto \sqrt{\Delta E / \Delta x}$

$$\Delta t \approx 100 \text{ ps}$$



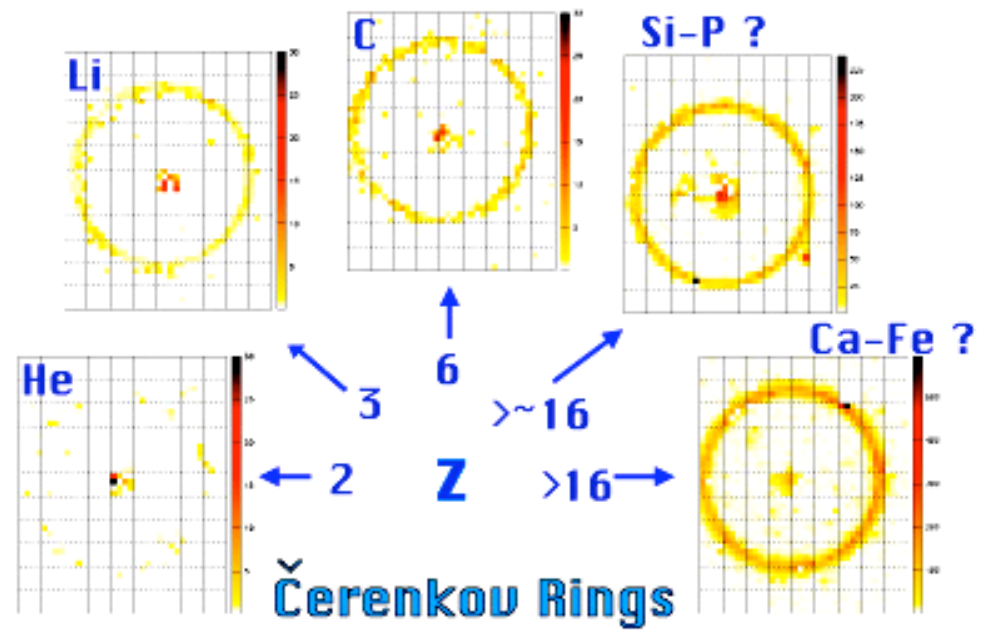
Ring Imaging Cerenkov counter RICH



RICH prototype

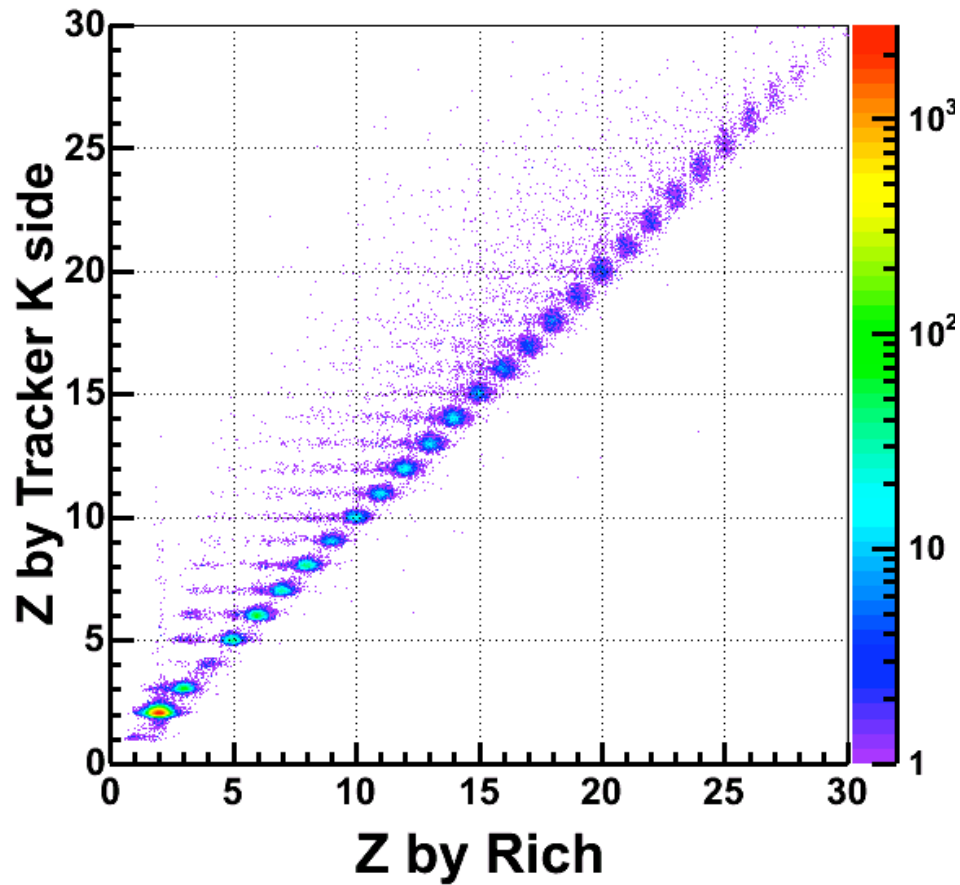


RICH - Test Beam Results

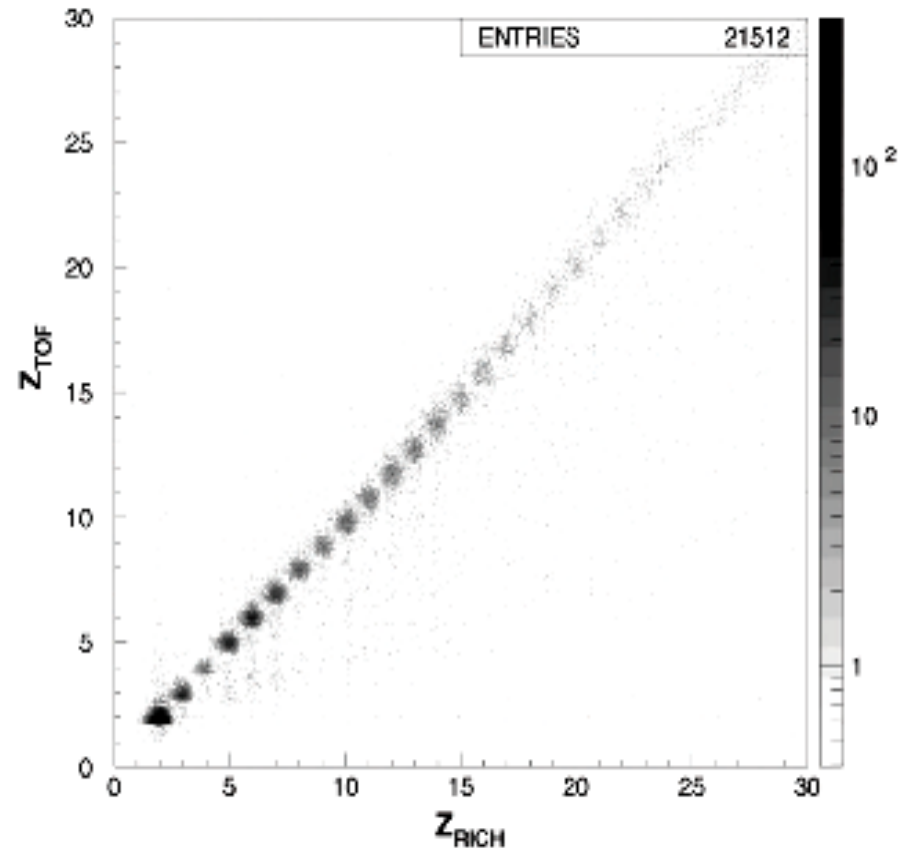


Z identification

TRK vs RICH



TOF vs RICH



$\bar{\text{He}}$ selection in AMS01

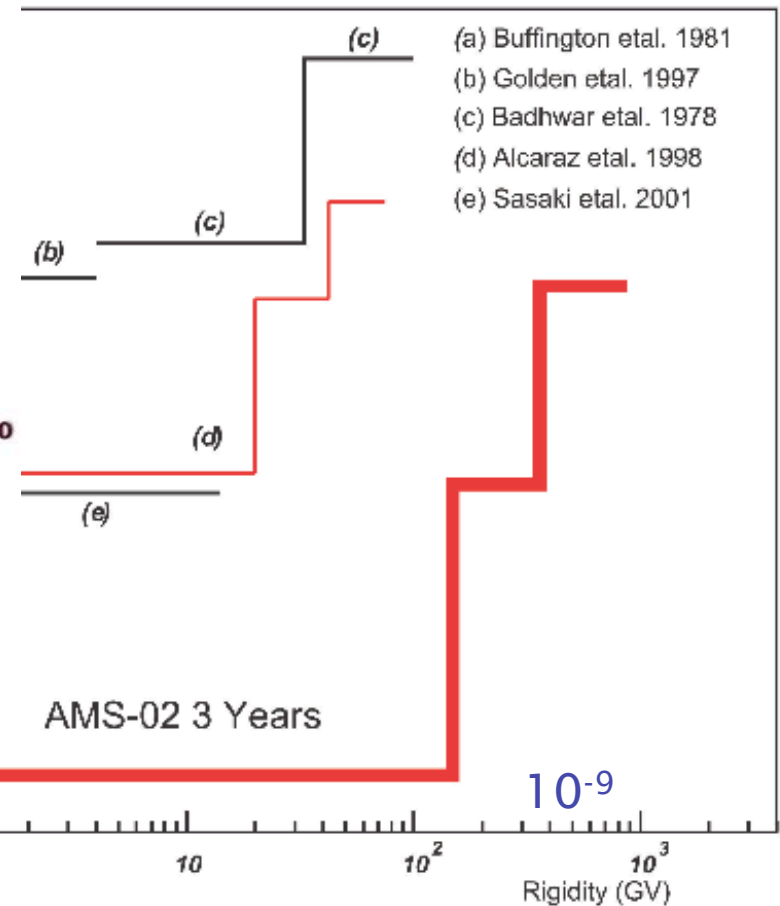
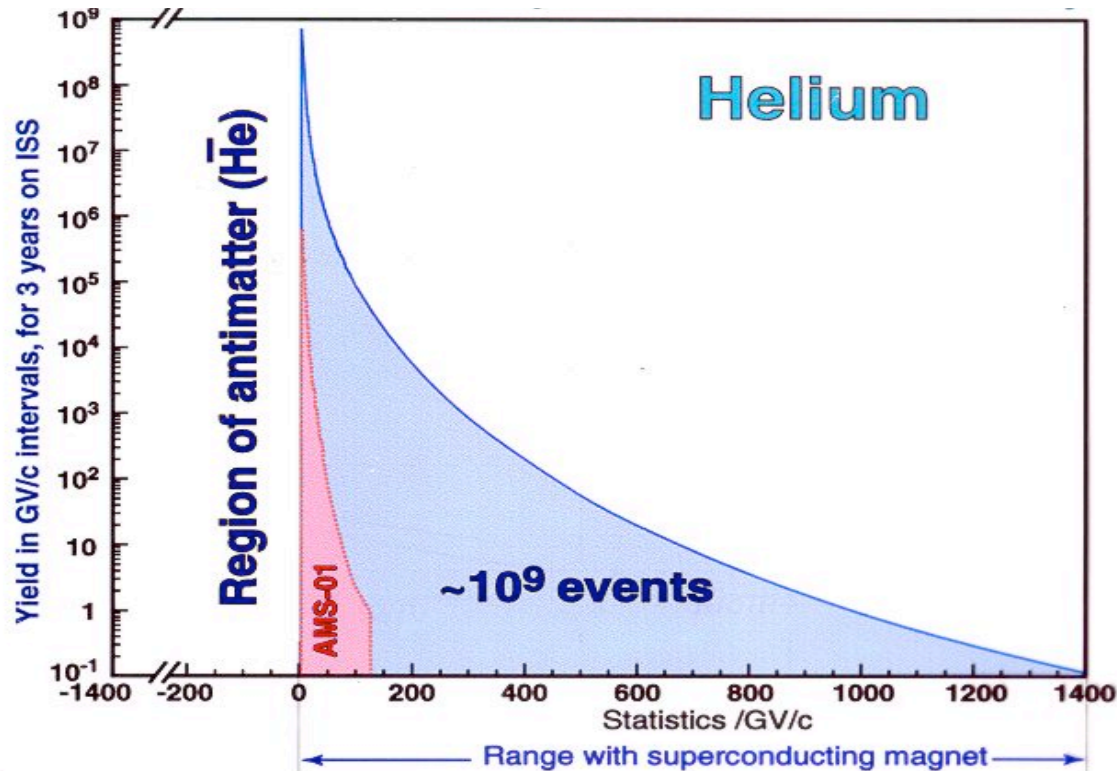
- track fits with 6, 5, 4 points out of 6 planes
- consistent charge sign in all fits
- χ^2 cut
- cuts on dE/dx in each plane to reject nuclear interactions
- kinematical fit to cut mass $< M_{\text{He}}$
- NO $\bar{\text{He}}$ candidates / 10^6 He ions

➔ AMS02: no false $\bar{\text{He}}$ / 10^9 He ions

AMS02 tracker has 8 planes

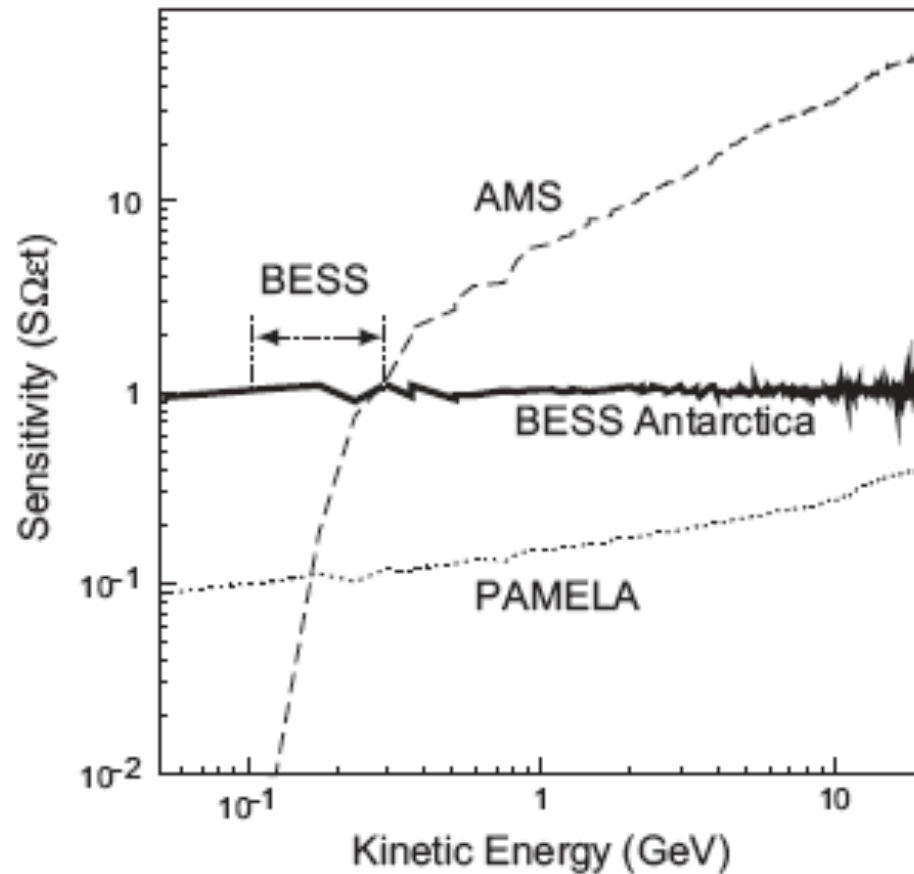
$$\text{BL}^2(\text{AMS02}) / \text{BL}^2(\text{AMS01}) = 6$$

AMS02 anti He limits



AMS-BESS-PAMELA

Confronto sensibilità tra gli esperimenti



area x angolo solido x tempo
esposizione

AMS02 volo 2010; t = 3 anni

BESS voli 2004, 2006-7; t = 20 gg

PAMELA volo 2007; t = 3 anni